



Taylor & Francis

Taylor & Francis Group

<http://taylorandfrancis.com>

Chapter 6

Array Theory – Linear Arrays

6.1 The Far-Field Beam Pattern of a Linear Array

An array can be thought of as a *sampled aperture*, that is, an aperture that is excited only at certain points or in certain localized areas. An array consists of individual electroacoustic transducers called *elements*. When an array is used in the *active mode*, the electroacoustic transducers are used as *transmitters*, converting electrical signals (voltages and currents) into acoustic signals (sound waves). When an array is used in the *passive mode*, the electroacoustic transducers are used as *receivers*, converting acoustic signals into electrical signals for further signal processing. In underwater acoustic applications, when an electroacoustic transducer is used as a transmitter, it is referred to as a *projector*, and when it is used as a receiver, it is referred to as a *hydrophone*. In seismic applications, an electroacoustic transducer used as a receiver is referred to as a *geophone*.

We know from complex aperture theory that an aperture function and its corresponding far-field beam pattern (directivity function) form a spatial Fourier transform pair. Therefore, since a linear array is an example of a linear aperture, the far-field beam pattern of a linear array lying along the X axis is given by the following one-dimensional spatial Fourier transform (see [Section 2.1](#)):

$$D(f, f_X) = F_{x_A} \{ A(f, x_A) \} = \int_{-\infty}^{\infty} A(f, x_A) \exp(+j2\pi f_X x_A) dx_A , \quad (6.1-1)$$

where $A(f, x_A)$ is the complex frequency response (complex aperture function) of the linear array, and

$$f_X = u/\lambda = \sin\theta \cos\psi/\lambda \quad (6.1-2)$$

is a spatial frequency in the X direction with units of cycles per meter. Since f_X can be expressed in terms of the spherical angles θ and ψ , the far-field beam pattern can ultimately be expressed as a function of frequency f and the spherical angles θ and ψ , that is, $D(f, f_X) \rightarrow D(f, \theta, \psi)$. We shall consider a field point to be in the far-field region of an array if the range r to the field point – as measured from the center of the array – satisfies the Fraunhofer (far-field) range criterion given by

$$r > \pi R_A^2 / \lambda > 2.414 R_A , \quad (6.1-3)$$

where R_A is the maximum radial extent of the array. If the overall length of the linear array is L_A meters, then $R_A = L_A/2$.

If a linear array lies along either the Y or Z axis instead of the X axis, then simply replace x_A and f_x with either y_A and f_y , or z_A and f_z , respectively, in (6.1-1), where spatial frequencies f_y and f_z are given by (1.2-44) and (1.2-45), respectively. As can be seen from (6.1-1), in order to derive the far-field beam pattern of a linear array, we must first specify a mathematical model for its complex frequency response.

6.1.1 Even Number of Elements

Consider a linear array composed of an *even* number of elements lying along the X axis, where each element is a single continuous line source or receiver L meters in length (see Fig. 6.1-1). If the elements are *not* identical, that is, if each element has a different complex frequency response, and if the elements are *not* equally spaced, as shown in Fig. 6.1-1, then the complex frequency response (complex aperture function) of this array can be expressed as

$$A(f, x_A) = \sum_{n=-N/2}^{-1} c_n(f) e_n(f, x_A - x_n) + \sum_{n=1}^{N/2} c_n(f) e_n(f, x_A - x_n), \quad (6.1-4)$$

or

$$A(f, x_A) = \sum_{n=1}^{N/2} [c_{-n}(f) e_{-n}(f, x_A - x_{-n}) + c_n(f) e_n(f, x_A - x_n)], \quad (6.1-5)$$

where N is the total even number of elements,

$c_n(f) = a_n(f) \exp[+j\theta_n(f)]$

(6.1-6)

is the frequency-dependent, *complex weight* associated with element n , $a_n(f)$ is a real, frequency-dependent, *dimensionless*, amplitude weight, $\theta_n(f)$ is a real, frequency-dependent, phase weight in radians, $e_n(f, x_A)$ is the complex frequency response (complex aperture function) of element n , also known as the *element function*, and x_n is the x coordinate of the center of element n . Note that because the elements are not equally spaced, $x_{-n} \neq -x_n$ in general. Complex weights are implemented by using digital signal processing (digital beamforming), as will be discussed in Section 6.4. Linear arrays of planar elements, such as rectangular and circular pistons, will be discussed in Chapter 8 (see Example 8.1-6).

Equation (6.1-4) indicates that the complex frequency response of the array is modeled as the sum (superposition) of the complex-weighted frequency responses of all the elements in the array. The complex weights are used to

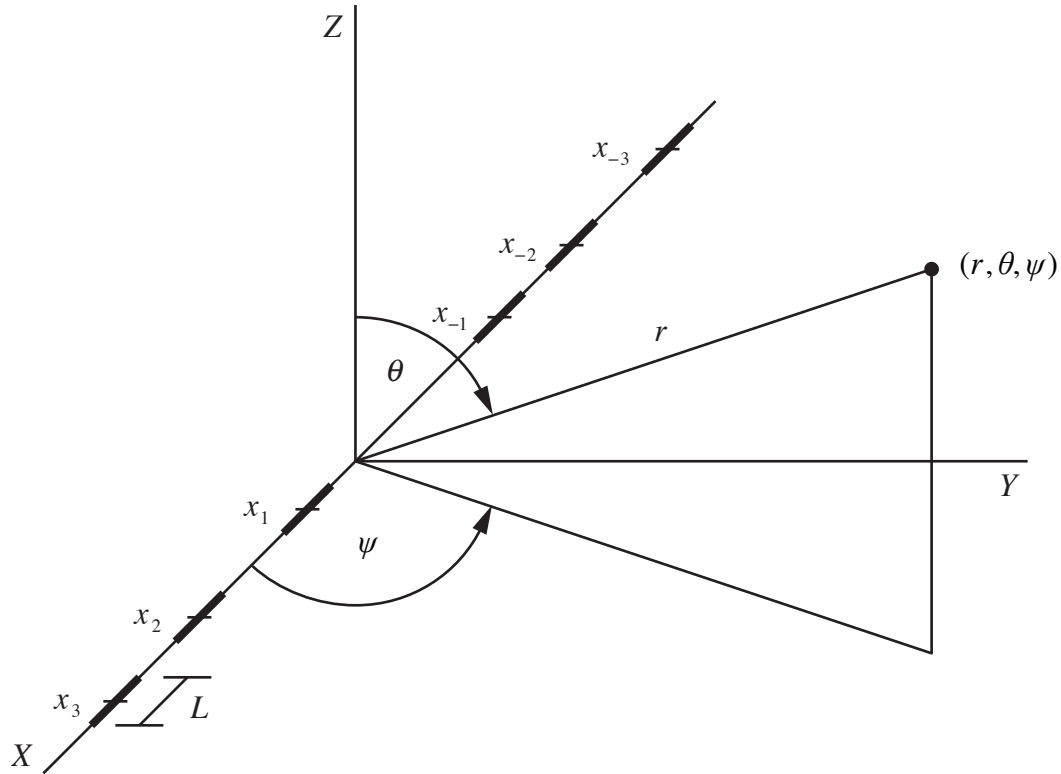


Figure 6.1-1 Linear array composed of an even number of unevenly-spaced, continuous line elements lying along the X axis. Each element is L meters in length. Also shown is a field point with spherical coordinates (r, θ, ψ) .

control the complex frequency response of the array and, thus, the array's far-field beam pattern via amplitude and phase weighting, as will be discussed later in this chapter. Substituting (6.1-5) into (6.1-1) yields the following expression for the far-field beam pattern:

$$D(f, f_X) = \sum_{n=1}^{N/2} [c_{-n}(f)E_{-n}(f, f_X)\exp(+j2\pi f_X x_{-n}) + c_n(f)E_n(f, f_X)\exp(+j2\pi f_X x_n)] \quad (6.1-7)$$

where

$$F_{x_A}\{e_n(f, x_A - x_n)\} = E_n(f, f_X)\exp(+j2\pi f_X x_n) \quad (6.1-8)$$

and

$$E_n(f, f_X) = F_{x_A}\{e_n(f, x_A)\} \quad (6.1-9)$$

is the far-field beam pattern of element (electroacoustic transducer) n . The units of $e_n(f, x_A)$, $A(f, x_A)$, $E_n(f, f_X)$, and $D(f, f_X)$ are summarized in [Table 6.1-1](#).

Table 6.1-1 Units of the Complex Frequency Responses $e_n(f, x_A)$ and $A(f, x_A)$ and Corresponding Far-Field Beam Patterns $E_n(f, f_X)$ and $D(f, f_X)$ for a Linear Array

Linear Array	$e_n(f, x_A)$, $A(f, x_A)$	$E_n(f, f_X)$, $D(f, f_X)$
active (transmit)	$(m^3/sec)/V$	$(m^3/sec)/V$
passive (receive)	$V/(m^2/sec)$	$V/(m^2/sec)$

If all the elements in the array are *identical* (i.e., all the elements have the same complex frequency response), but still *not* equally spaced, then (6.1-7) reduces to

$$D(f, f_X) = E(f, f_X)S(f, f_X) \quad (6.1-10)$$

where

$$E(f, f_X) = F_{x_A} \{ e(f, x_A) \} \quad (6.1-11)$$

is the far-field beam pattern of *one* of the identical elements in the array,

$$S(f, f_X) = \sum_{n=1}^{N/2} [c_{-n}(f) \exp(+j2\pi f_X x_{-n}) + c_n(f) \exp(+j2\pi f_X x_n)] \quad (6.1-12)$$

is the *array factor*, and if $a_{-n}(f) > 0$ and $a_n(f) > 0 \ \forall n$, then

$$S_{\max} = \max |S(f, f_X)| = \sum_{n=1}^{N/2} [a_{-n}(f) + a_n(f)] \quad (6.1-13)$$

is the *normalization factor* for the array factor (see [Appendix 6A](#)). As can be seen from (6.1-12), $S(f, f_X)$ is *dimensionless* and depends on the set of complex weights used and the locations (the x coordinates) of all the elements along the X axis. The array factor $S(f, f_X)$ contains the spatial information of the array. If one or more elements in the array are broken (not transmitting and/or receiving), set $c_n(f) = 0$ for those elements.

Equation (6.1-10) is referred to as the *Product Theorem* for a linear array composed of an even number of identical elements. The Product Theorem states that the far-field beam pattern $D(f, f_X)$ of a linear array composed of an even number of *identical*, unevenly-spaced, complex-weighted elements is equal to the *product* of the far-field beam pattern $E(f, f_X)$ of *one* of the identical elements in the array, and the dimensionless array factor $S(f, f_X)$, which is related to the far-field beam pattern of an equivalent linear array composed of an even number of identical, unevenly-spaced, complex-weighted, *omnidirectional point-elements*. Although the Product Theorem requires identical elements, equal spacing of the elements is *not* required. The interpretation of $S(f, f_X)$ shall be discussed next.

In acoustic wave-propagation theory, an impulse function is used as a mathematical model for an omnidirectional point-source. Similarly, the mathematical model that we shall use for the complex frequency response of an omnidirectional point-element lying along the X axis is given by

$$e(f, x_A) = \mathcal{S}(f) \delta(x_A), \quad (6.1-14)$$

where $\mathcal{S}(f)$ is the complex, *element sensitivity function*. A real-world example of an omnidirectional point-element is a spherical sound-source manufactured to vibrate in the monopole mode of vibration and whose circumference is small compared to a wavelength. If the point-element is used in the active mode as a transmitter, then the element sensitivity function $\mathcal{S}(f)$ is referred to as the *transmitter sensitivity function* with units of $(m^3/sec)/V$ (see [Appendix 6B](#)). If the point-element is used in the passive mode as a receiver, then $\mathcal{S}(f)$ is referred to as the *receiver sensitivity function* with units of $V/(m^2/sec)$ (see [Appendix 6B](#)). Note that $\int_{-\infty}^{\infty} e(f, x_A) dx_A = \mathcal{S}(f)$ because $\int_{-\infty}^{\infty} \delta(x_A) dx_A = 1$ (see [Appendix 6C](#)). The impulse function $\delta(x_A)$ has units of inverse meters. The units of $\mathcal{S}(f)$ are summarized in [Table 6.1-2](#).

Table 6.1-2 Units of the Element Sensitivity Function $\mathcal{S}(f)$

Omnidirectional Point-Element	$\mathcal{S}(f)$
active (transmit)	$(m^3/sec)/V$
passive (receive)	$V/(m^2/sec)$

Since

$$F_{x_A}\{\delta(x_A)\} = 1, \quad (6.1-15)$$

taking the spatial Fourier transform of (6.1-14) yields

$$E(f, f_X) = \mathcal{S}(f). \quad (6.1-16)$$

Equation (6.1-16) is the far-field beam pattern of an omnidirectional point-element, and as expected, it is *not* a function of the spherical angles θ and ψ . The term “omnidirectional” means that an electroacoustic transducer transmits and/or receives equally well in all directions. Therefore, by substituting (6.1-16) into (6.1-10), we obtain the following expression for the far-field beam pattern of a linear array composed of an even number of identical, unevenly-spaced, complex-weighted, omnidirectional point-elements lying along the X axis:

$$D(f, f_X) = \mathcal{S}(f)S(f, f_X) \quad (6.1-17)$$

where $S(f, f_X)$ is given by (6.1-12). The corresponding complex frequency response (complex aperture function) of the array can be obtained by taking the inverse spatial Fourier transform of (6.1-17). Doing so yields

$$A(f, x_A) = \mathcal{S}(f) \sum_{n=1}^{N/2} [c_{-n}(f)\delta(x_A - x_{-n}) + c_n(f)\delta(x_A - x_n)] \quad (6.1-18)$$

since

$$F_{f_X}^{-1}\{\exp(+j2\pi f_X x_n)\} = \delta(x_A - x_n). \quad (6.1-19)$$

Note that the summation in (6.1-18) is in the form of the impulse response of a finite impulse response (FIR) digital filter. In [Appendix 6D](#), it is shown that a linear array composed of an even number of identical, complex-weighted elements can be thought of as a one-dimensional, spatial FIR filter, where $s(f, x_A) = F_{f_X}^{-1}\{S(f, f_X)\}$ is the spatial impulse response of the array at frequency f hertz.

If all the elements in the array are *equally spaced*, then

$$x_n = (n - 0.5)d, \quad n = 1, 2, \dots, N/2 \quad (6.1-20)$$

and

$$x_{-n} = -x_n, \quad n = 1, 2, \dots, N/2 \quad (6.1-21)$$

where d is the *interelement spacing* in meters.

If all the elements in the array are equally spaced and the complex weights satisfy the conjugate symmetry property

$$c_{-n}(f) = c_n^*(f), \quad n = 1, 2, \dots, N/2, \quad (6.1-22)$$

where the asterisk denotes complex conjugate, then the array factor $S(f, f_x)$ given by (6.1-12) can be simplified. Before we begin the procedure of simplifying $S(f, f_x)$, let us first examine the consequences of (6.1-22). Substituting (6.1-6) into (6.1-22) yields

$$a_{-n}(f) \exp[+j\theta_{-n}(f)] = a_n(f) \exp[-j\theta_n(f)], \quad n = 1, 2, \dots, N/2, \quad (6.1-23)$$

from which we obtain the following two equations:

$$a_{-n}(f) = a_n(f), \quad n = 1, 2, \dots, N/2, \quad (6.1-24)$$

and

$$\theta_{-n}(f) = -\theta_n(f), \quad n = 1, 2, \dots, N/2. \quad (6.1-25)$$

Equations (6.1-24) and (6.1-25) indicate that if the complex weights satisfy the conjugate symmetry property given by (6.1-22), then the amplitude and phase weights are *even* and *odd* functions of index n , respectively.

We begin the procedure of simplifying $S(f, f_x)$ by substituting (6.1-20) through (6.1-22) into (6.1-12) which yields

$$\begin{aligned} S(f, f_x) &= \sum_{n=1}^{N/2} \left[c_n^*(f) \exp[-j2\pi f_x(n-0.5)d] + c_n(f) \exp[+j2\pi f_x(n-0.5)d] \right] \\ &= \sum_{n=1}^{N/2} \left\{ [c_n(f) \exp[+j2\pi f_x(n-0.5)d]]^* + [c_n(f) \exp[+j2\pi f_x(n-0.5)d]] \right\}. \end{aligned} \quad (6.1-26)$$

Since $Z^* + Z = 2 \operatorname{Re}\{Z\}$, (6.1-26) reduces to

$$S(f, f_x) = 2 \sum_{n=1}^{N/2} \operatorname{Re}\{c_n(f) \exp[+j2\pi f_x(n-0.5)d]\}, \quad (6.1-27)$$

and by substituting (6.1-6) into (6.1-27), we finally obtain

$$S(f, f_x) = 2 \sum_{n=1}^{N/2} a_n(f) \cos[2\pi f_x(n-0.5)d + \theta_n(f)] \quad (6.1-28)$$

Equation (6.1-28) is valid only if all the identical elements in the array are equally spaced and the complex weights satisfy the conjugate symmetry property given by (6.1-22).

Example 6.1-1 Two-Element Interferometer

A *two-element interferometer* is a linear array of two identical, complex-weighted, omnidirectional point-elements that are equally spaced about the origin of the coordinate system (the center of the array as shown in Fig. 6.1-2) where the complex weights satisfy the conjugate symmetry property given by (6.1-22). Since the elements are equally spaced, substituting $N = 2$ into (6.1-20) and (6.1-21) yields the following x coordinates of the centers of the two elements:

$$x_1 = d/2 \quad (6.1-29)$$

and

$$x_{-1} = -x_1 = -d/2 \quad (6.1-30)$$

so that the interelement spacing is d meters. Since the complex weights satisfy the conjugate symmetry property given by (6.1-22), substituting $N = 2$ into (6.1-24) and (6.1-25) yields

$$a_{-1}(f) = a_1(f) \quad (6.1-31)$$

and

$$\theta_{-1}(f) = -\theta_1(f). \quad (6.1-32)$$

And since the elements are identical, substituting $N = 2$ into (6.1-28), and then substituting the result into (6.1-17) yields

$$D(f, f_x) = 2a_1(f)\mathcal{S}(f)\cos[\pi f_x d + \theta_1(f)] \quad (6.1-33)$$

where $\mathcal{S}(f)$ is the complex, element sensitivity function. Equation (6.1-33) is the *unnormalized*, far-field beam pattern of a two-element interferometer lying along the X axis.

The *dimensionless, normalized*, far-field beam pattern is defined as follows:

$$D_N(f, f_x) \triangleq D(f, f_x)/D_{\max} \quad (6.1-34)$$

where $D_{\max} = \max|D(f, f_x)|$ is the *normalization factor* – it is the *maximum* value of the *magnitude* of the unnormalized, far-field beam pattern. Therefore, by referring to (6.1-33),

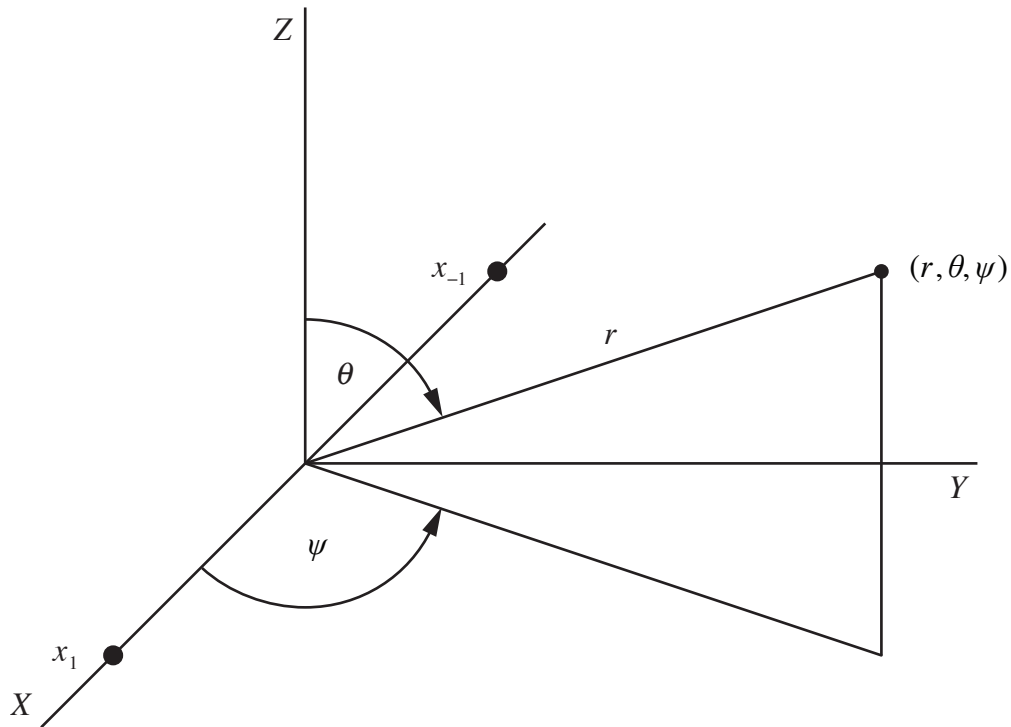


Figure 6.1-2 Linear array of two omnidirectional point-elements lying along the X axis. Also shown is a field point with spherical coordinates (r, θ, ψ) .

$$|D(f, f_x)| = 2 |a_1(f)| |\mathcal{S}(f)| |\cos[\pi f_x d + \theta_1(f)]|, \quad (6.1-35)$$

and since the maximum value of the magnitude of a cosine function is 1,

$$D_{\max} = 2 |a_1(f)| |\mathcal{S}(f)|. \quad (6.1-36)$$

Dividing (6.1-35) by (6.1-36) yields the following expression for the magnitude of the *normalized*, far-field beam pattern of a two-element interferometer lying along the X axis:

$|D_N(f, f_x)| = |\cos[\pi f_x d + \theta_1(f)]| \quad (6.1-37)$

Because we have not yet discussed phase weights in any great detail, let $\theta_1(f) = 0$. In other words, if only amplitude weighting is done (no phase weighting), then (6.1-37) reduces to

$$|D_N(f, f_x)| = |\cos(\pi f_x d)|. \quad (6.1-38)$$

Since spatial frequency

$$f_x = u/\lambda = \sin \theta \cos \psi / \lambda, \quad (6.1-39)$$

(6.1-38) can also be expressed as

$$|D_N(f, u)| = \left| \cos\left(\pi \frac{d}{\lambda} u\right) \right|, \quad (6.1-40)$$

or

$$|D_N(f, \theta, \psi)| = \left| \cos\left(\pi \frac{d}{\lambda} \sin \theta \cos \psi\right) \right|. \quad (6.1-41)$$

At broadside, where direction cosine $u = 0$, (6.1-40) reduces to $|D_N(f, 0)| = 1$, and by setting $\theta = 90^\circ$ in (6.1-41), we obtain

$$|D_N(f, 90^\circ, \psi)| = \left| \cos\left(\pi \frac{d}{\lambda} \cos \psi\right) \right|, \quad (6.1-42)$$

which is the magnitude of the normalized, *horizontal*, far-field beam pattern in the *XY* plane of a two-element interferometer lying along the *X* axis (see Fig. 6.1-3).

As can be seen in Fig. 6.1-3, the main lobe exists on both the port and starboard (left and right) sides of the array. This is an example of the *port/starboard (left/right) ambiguity problem* associated with linear arrays since a target at broadside on the port side will produce the same output electrical signal from the array as a target at broadside on the starboard side. Solutions to the port/starboard (left/right) ambiguity problem are discussed in Chapters 8 and 9, Examples 8.2-1 and 9.1-2, respectively. ■

Example 6.1-2 Dipole

A *dipole* is a linear array of two identical, complex-weighted, omnidirectional point-elements that are equally spaced about the origin of the coordinate system (the center of the array as shown in Fig. 6.1-2) where the complex weights do *not* satisfy the conjugate symmetry property given by (6.1-22). Since the elements are equally spaced, substituting $N = 2$ into (6.1-20) and (6.1-21) yields the following x coordinates of the centers of the two elements:

$$x_1 = d/2 \quad (6.1-43)$$

and

$$x_{-1} = -x_1 = -d/2 \quad (6.1-44)$$

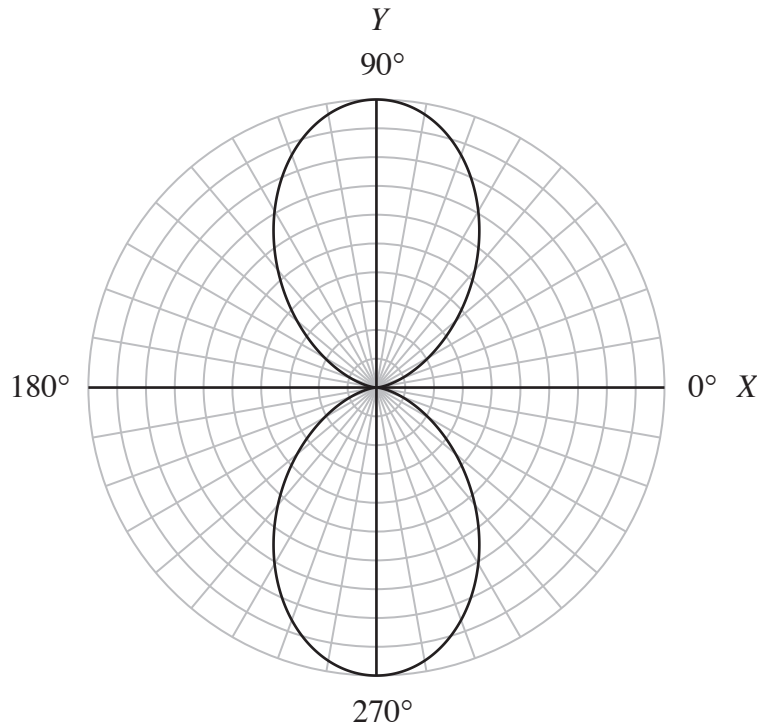


Figure 6.1-3 Polar plot, as a function of the azimuthal (bearing) angle ψ , of the magnitude of the normalized, horizontal, far-field beam pattern of a two-element interferometer lying along the X axis given by (6.1-42) for $d/\lambda = 0.5$.

so that the interelement spacing is d meters. In a dipole, *both* the amplitude and phase weights have *odd* symmetry, that is,

$$a_{-l}(f) = -a_l(f) \quad (6.1-45)$$

and

$$\theta_{-l}(f) = -\theta_l(f). \quad (6.1-46)$$

And since the elements are identical, substituting $N = 2$, (6.1-6), and (6.1-43) through (6.1-46) into (6.1-12) yields

$$S(f, f_X) = a_l(f) [\exp\{+j[\pi f_X d + \theta_l(f)]\} - \exp\{-j[\pi f_X d + \theta_l(f)]\}], \quad (6.1-47)$$

which reduces to

$$S(f, f_X) = j 2 a_l(f) \sin[\pi f_X d + \theta_l(f)]. \quad (6.1-48)$$

Substituting (6.1-48) into (6.1-17) yields

$$D(f, f_x) = j2a_1(f)\mathcal{S}(f)\sin[\pi f_x d + \theta_1(f)] \quad (6.1-49)$$

where $\mathcal{S}(f)$ is the complex, element sensitivity function. Equation (6.1-49) is the *unnormalized*, far-field beam pattern of a dipole lying along the X axis.

The magnitude of the far-field beam pattern given by (6.1-49) is

$$|D(f, f_x)| = 2|a_1(f)| |\mathcal{S}(f)| |\sin[\pi f_x d + \theta_1(f)]|, \quad (6.1-50)$$

and since the maximum value of the magnitude of a sine function is 1,

$$D_{\max} = 2|a_1(f)| |\mathcal{S}(f)|. \quad (6.1-51)$$

Dividing (6.1-50) by (6.1-51) yields the following expression for the magnitude of the *normalized*, far-field beam pattern of a dipole lying along the X axis:

$$|D_N(f, f_x)| = |\sin[\pi f_x d + \theta_1(f)]| \quad (6.1-52)$$

If we let $\theta_1(f) = 0$, that is, if only amplitude weighting is done (no phase weighting), then (6.1-52) reduces to

$$|D_N(f, f_x)| = |\sin(\pi f_x d)|. \quad (6.1-53)$$

Since spatial frequency

$$f_x = u/\lambda = \sin\theta \cos\psi/\lambda, \quad (6.1-54)$$

(6.1-53) can also be expressed as

$$|D_N(f, u)| = \left| \sin\left(\pi \frac{d}{\lambda} u\right) \right|, \quad (6.1-55)$$

or

$$|D_N(f, \theta, \psi)| = \left| \sin\left(\pi \frac{d}{\lambda} \sin\theta \cos\psi\right) \right|. \quad (6.1-56)$$

At broadside, where direction cosine $u = 0$, (6.1-55) reduces to $|D_N(f, 0)| = 0$, and by setting $\theta = 90^\circ$ in (6.1-56), we obtain

$$|D_N(f, 90^\circ, \psi)| = \left| \sin\left(\pi \frac{d}{\lambda} \cos\psi\right) \right|, \quad (6.1-57)$$

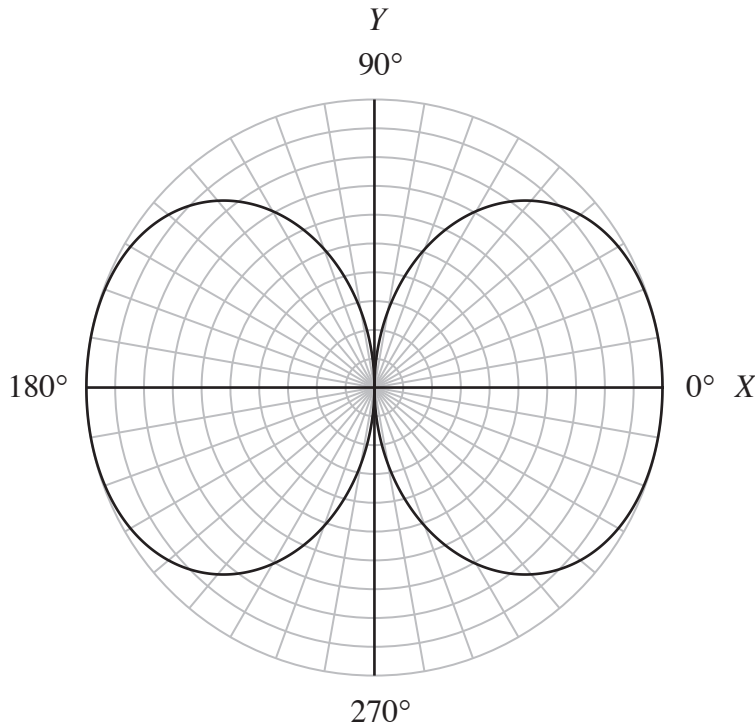


Figure 6.1-4 Polar plot, as a function of the azimuthal (bearing) angle ψ , of the magnitude of the normalized, horizontal, far-field beam pattern of a dipole lying along the X axis given by (6.1-57) for $d/\lambda = 0.5$.

which is the magnitude of the normalized, *horizontal*, far-field beam pattern in the XY plane of a dipole lying along the X axis (see Fig. 6.1-4). Unlike the far-field beam pattern of a two-element interferometer which has a maximum at broadside (see Fig. 6.1-3), the dipole has a null.

Example 6.1-3 Cardioid Beam Pattern

Consider a linear array of two identical, complex-weighted, omni-directional point-elements that are equally spaced about the origin of the coordinate system (the center of the array as shown in Fig. 6.1-2). Since the elements are equally spaced, substituting $N = 2$ into (6.1-20) and (6.1-21) yields the following x coordinates of the centers of the two elements:

$$x_1 = d/2 \quad (6.1-58)$$

and

$$x_{-1} = -x_1 = -d/2 \quad (6.1-59)$$

so that the interelement spacing is d meters. The amplitude weights are equal, that is,

$$a_{-1}(f) = a_1(f), \quad (6.1-60)$$

and the phase weights are

$$\theta_1(f) = 0 \quad (6.1-61)$$

and

$$\theta_{-1}(f) = \pi/2. \quad (6.1-62)$$

Substituting (6.1-60) through (6.1-62) into (6.1-6) yields the following complex weights:

$$c_1(f) = a_1(f) \quad (6.1-63)$$

and

$$c_{-1}(f) = a_1(f) \exp(+j\pi/2) = ja_1(f). \quad (6.1-64)$$

Substituting $N = 2$, (6.1-58), (6.1-59), (6.1-63), and (6.1-64) into (6.1-12) yields the array factor

$$S(f, f_x) = a_1(f) [j \exp(-j\pi f_x d) + \exp(+j\pi f_x d)]. \quad (6.1-65)$$

If the interelement spacing

$$d = \lambda/4, \quad (6.1-66)$$

and since spatial frequency

$$f_x = u/\lambda = \sin \theta \cos \psi / \lambda, \quad (6.1-67)$$

the array factor given by (6.1-65) can be rewritten as

$$S(f, u) = (1+j)a_1(f) [\cos(\pi u/4) + \sin(\pi u/4)], \quad (6.1-68)$$

or

$$S(f, u) = \sqrt{2}(1+j)a_1(f) \cos[\pi(u-1)/4], \quad (6.1-69)$$

since

$$\cos \alpha + \sin \alpha = \sqrt{2} \cos[\alpha - (\pi/4)]. \quad (6.1-70)$$

And since the elements are identical, the *unnormalized*, far-field beam pattern of the array is given by [see (6.1-17)]

$$D(f, u) = \sqrt{2} (1+j) a_1(f) \mathcal{S}(f) \cos[\pi(u-1)/4] \quad (6.1-71)$$

where $\mathcal{S}(f)$ is the complex, element sensitivity function.

The magnitude of the far-field beam pattern given by (6.1-71) is

$$|D(f, u)| = 2 |a_1(f)| |\mathcal{S}(f)| |\cos[\pi(u-1)/4]|, \quad (6.1-72)$$

and since the maximum value of $|\cos[\pi(u-1)/4]|$ occurs at $u=1$ where $|\cos(0)|=1$, the normalization factor is

$$D_{\max} = \max |D(f, u)| = 2 |a_1(f)| |\mathcal{S}(f)|. \quad (6.1-73)$$

Dividing (6.1-72) by (6.1-73) yields the following expression for the magnitude of the *normalized*, far-field beam pattern:

$$|D_N(f, u)| = |\cos[\pi(u-1)/4]| \quad (6.1-74)$$

where $|D_N(f, 1)|=1$. Substituting $u = \sin\theta \cos\psi$ into (6.1-74) yields

$$|D_N(f, \theta, \psi)| = \left| \cos \left[\frac{\pi}{4} (\sin\theta \cos\psi - 1) \right] \right|, \quad (6.1-75)$$

and by setting $\theta = 90^\circ$ in (6.1-75), we obtain

$$|D_N(f, 90^\circ, \psi)| = \left| \cos \left[\frac{\pi}{4} (\cos\psi - 1) \right] \right|, \quad (6.1-76)$$

which is the magnitude of the normalized, *horizontal*, far-field beam pattern in the XY plane (see Fig. 6.1-5). The beam pattern shown in Fig. 6.1-5 is referred to as a *cardioid* (heart-shaped) beam pattern. The main lobe is aligned along the positive X axis since the maximum value of the normalized beam pattern occurs at $u=1$, which is one of the end-fire locations in direction-cosine space for a linear array lying along the X axis.

If the following set of phase weights are used instead,

$$\theta_1(f) = 0 \quad (6.1-77)$$

and

$$\theta_{-1}(f) = -\pi/2, \quad (6.1-78)$$

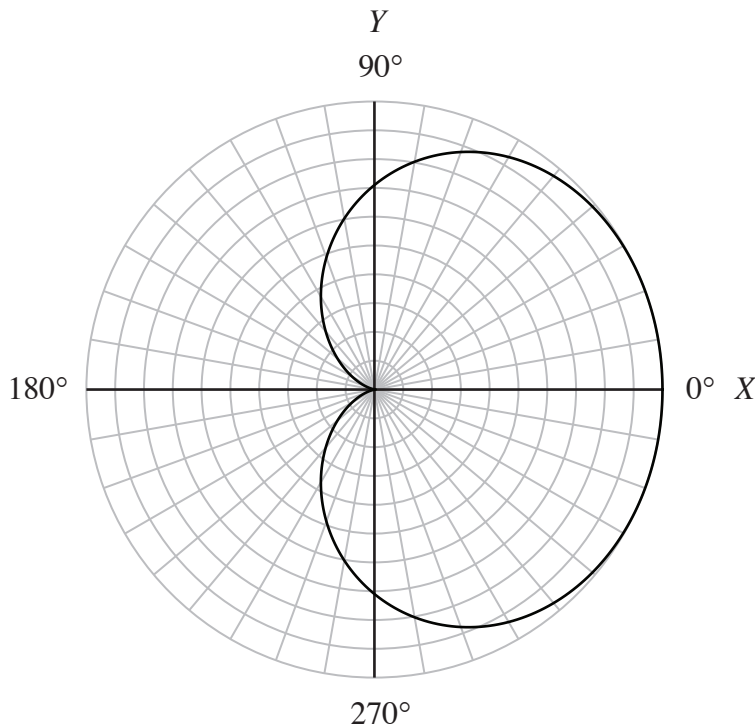


Figure 6.1-5 Polar plot, as a function of the azimuthal (bearing) angle ψ , of the magnitude of the normalized, horizontal, far-field beam pattern given by (6.1-76).

then the *unnormalized*, far-field beam pattern is given by

$$D(f, u) = \sqrt{2}(1-j)a_1(f)\mathcal{S}(f)\cos[\pi(u+1)/4] \quad (6.1-79)$$

the magnitude of the *normalized*, far-field beam pattern is given by

$$|D_N(f, u)| = |\cos[\pi(u+1)/4]| \quad (6.1-80)$$

or

$$|D_N(f, \theta, \psi)| = \left| \cos\left[\frac{\pi}{4}(\sin \theta \cos \psi + 1)\right] \right|, \quad (6.1-81)$$

and by setting $\theta = 90^\circ$ in (6.1-81), we obtain

$$|D_N(f, 90^\circ, \psi)| = \left| \cos\left[\frac{\pi}{4}(\cos \psi + 1)\right] \right|, \quad (6.1-82)$$

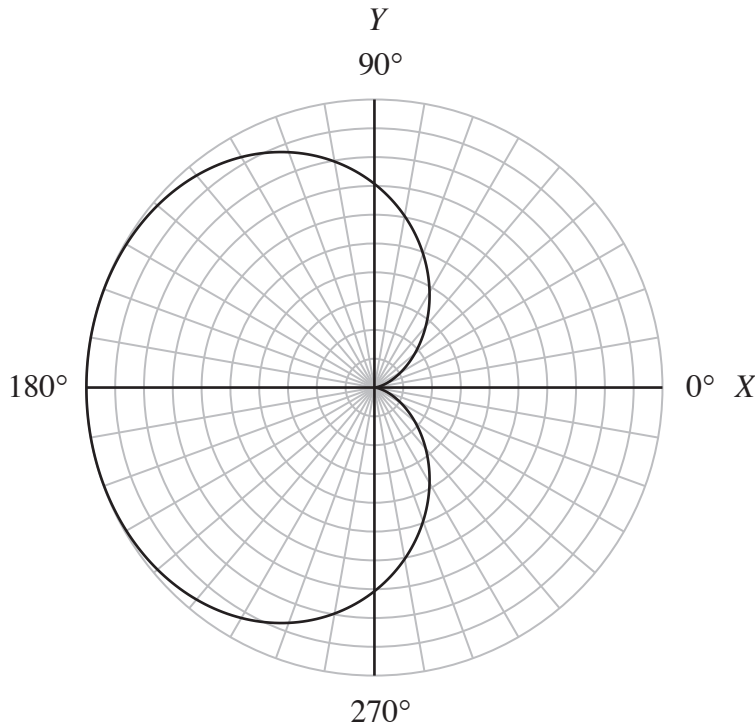


Figure 6.1-6 Polar plot, as a function of the azimuthal (bearing) angle ψ , of the magnitude of the normalized, horizontal, far-field beam pattern given by (6.1-82).

which is the magnitude of the normalized, *horizontal*, far-field beam pattern in the *XY* plane (see Fig. 6.1-6). The main lobe is now aligned along the negative *X* axis since the maximum value of the normalized beam pattern occurs at $u = -1$, which is the other end-fire location in direction-cosine space for a linear array lying along the *X* axis. The *triplet circular array* discussed in Example 8.1-7 also has a cardioid far-field beam pattern. ■

6.1.2 Odd Number of Elements

Consider a linear array composed of an *odd* number of elements lying along the *X* axis, where each element is a single continuous line source or receiver *L* meters in length (see Fig. 6.1-7). If the elements are *not* identical, that is, if each element has a different complex frequency response, and if the elements are *not* equally spaced, as shown in Fig. 6.1-7, then the complex frequency response (complex aperture function) of this array can be expressed as

$$A(f, x_A) = \sum_{n=-N'}^{N'} c_n(f) e_n(f, x_A - x_n), \quad (6.1-83)$$

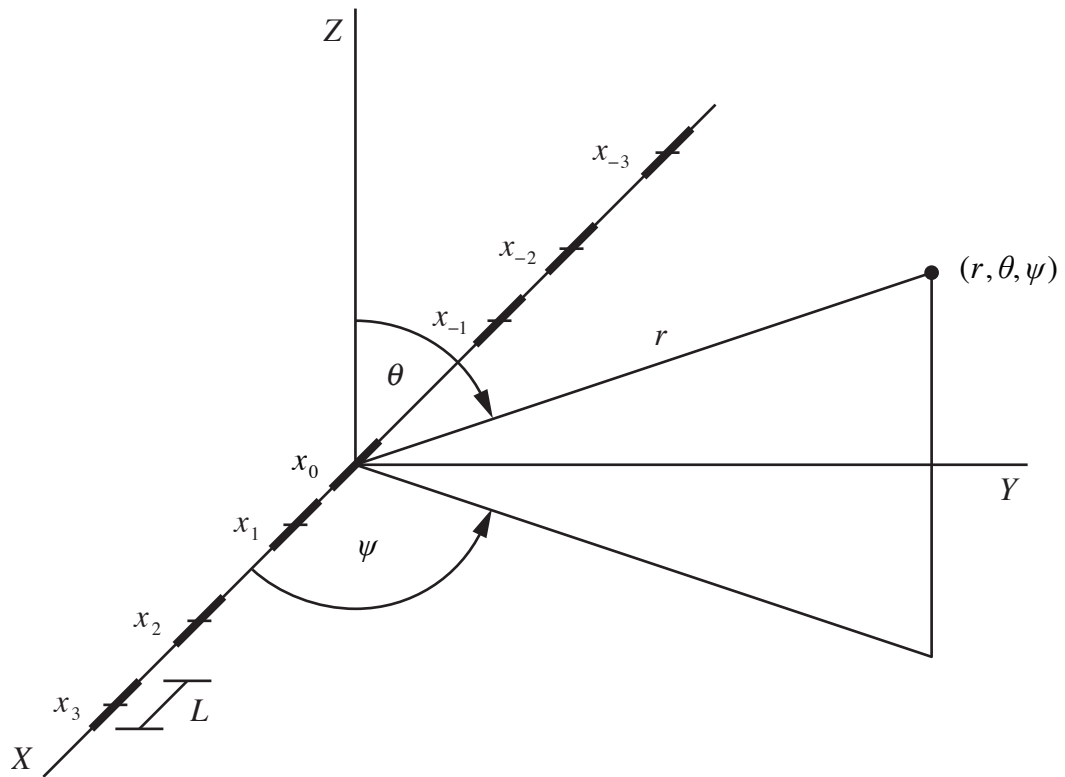


Figure 6.1-7 Linear array composed of an odd number of unevenly-spaced, continuous line elements lying along the X axis. Each element is L meters in length. Also shown is a field point with spherical coordinates (r, θ, ψ) .

where

$$N' = (N-1)/2 , \quad (6.1-84)$$

N is the total odd number of elements, $c_n(f)$ is the frequency-dependent, complex weight associated with element n [see (6.1-6)], $e_n(f, x_A)$ is the complex frequency response (complex aperture function) of element n , also known as the element function, and x_n is the x coordinate of the center of element n . Note that $x_0 = 0$ because element $n=0$ is centered at the origin of the coordinate system, and because the elements are not equally spaced, $x_{-n} \neq -x_n$ in general. As was mentioned in Subsection 6.1.1, complex weights are implemented by using digital signal processing (digital beamforming) (see Section 6.4), and linear arrays of planar elements, such as rectangular and circular pistons, will be discussed in Chapter 8 (see Example 8.1-8).

Equation (6.1-83) indicates that the complex frequency response of the array is modeled as the sum (superposition) of the complex-weighted frequency

responses of all the elements in the array. The complex weights are used to control the complex frequency response of the array and, thus, the array's far-field beam pattern via amplitude and phase weighting, as will be discussed later in this chapter. Substituting (6.1-83) into (6.1-1) yields the following expression for the far-field beam pattern:

$$D(f, f_X) = \sum_{n=-N'}^{N'} c_n(f) E_n(f, f_X) \exp(+j2\pi f_X x_n) \quad (6.1-85)$$

where $E_n(f, f_X)$ is the far-field beam pattern of element (electroacoustic transducer) n [see (6.1-8) and (6.1-9)]. The units of $e_n(f, x_A)$, $A(f, x_A)$, $E_n(f, f_X)$, and $D(f, f_X)$ are summarized in [Table 6.1-1](#).

If all the elements in the array are *identical* (i.e., all the elements have the same complex frequency response), but still *not* equally spaced, then (6.1-85) reduces to

$$D(f, f_X) = E(f, f_X) S(f, f_X) \quad (6.1-86)$$

where $E(f, f_X)$ is the far-field beam pattern of *one* of the identical elements in the array [see (6.1-11)],

$$S(f, f_X) = \sum_{n=-N'}^{N'} c_n(f) \exp(+j2\pi f_X x_n) \quad (6.1-87)$$

is the *array factor*, and if $a_n(f) > 0 \quad \forall n$, then

$$S_{\max} = \max |S(f, f_X)| = \sum_{n=-N'}^{N'} a_n(f) \quad (6.1-88)$$

is the *normalization factor* for the array factor (see [Appendix 6A](#)). As can be seen from (6.1-87), $S(f, f_X)$ is *dimensionless* and depends on the set of complex weights used and the locations (the x coordinates) of all the elements along the X axis. The array factor $S(f, f_X)$ contains the spatial information of the array. If one or more elements in the array are broken (not transmitting and/or receiving), set $c_n(f) = 0$ for those elements. Equation (6.1-86) is referred to as the *Product Theorem* for a linear array composed of an odd number of identical elements. It has the same form and meaning as the Product Theorem for a linear array composed of an even number of identical elements given by (6.1-10), with the exception that the equations for the array factor $S(f, f_X)$ are different – compare

(6.1-12) with (6.1-87).

If the identical elements in the array are omnidirectional point-elements, then substituting (6.1-16) into (6.1-86) yields

$$D(f, f_x) = \mathcal{S}(f) S(f, f_x) \quad (6.1-89)$$

where $\mathcal{S}(f)$ is the complex, element sensitivity function (see [Table 6.1-2](#) and [Appendix 6B](#)), and $S(f, f_x)$ is given by (6.1-87). The corresponding complex frequency response (complex aperture function) of the array can be obtained by taking the inverse spatial Fourier transform of (6.1-89). Doing so yields [see (6.1-19)]

$$A(f, x_A) = \mathcal{S}(f) \sum_{n=-N'}^{N'} c_n(f) \delta(x_A - x_n) \quad (6.1-90)$$

Note that the summation in (6.1-90) is in the form of the impulse response of a finite impulse response (FIR) digital filter. In [Appendix 6D](#), it is shown that a linear array composed of an odd number of identical, complex-weighted elements can be thought of as a one-dimensional, spatial FIR filter, where $s(f, x_A) = F_{f_x}^{-1}\{S(f, f_x)\}$ is the spatial impulse response of the array at frequency f hertz.

If all the elements in the array are *equally spaced*, then

$$x_n = nd, \quad n = -N', \dots, 0, \dots, N' \quad (6.1-91)$$

and

$$x_{-n} = -x_n, \quad n = 1, \dots, N' \quad (6.1-92)$$

where d is the *interelement spacing* in meters.

If all the elements in the array are equally spaced and the complex weights satisfy the conjugate symmetry property

$$c_{-n}(f) = c_n^*(f), \quad n = 1, 2, \dots, N', \quad (6.1-93)$$

then the array factor $S(f, f_x)$ given by (6.1-87) can be simplified. As was discussed before [see (6.1-22) through (6.1-25)], (6.1-93) implies that the amplitude and phase weights are even and odd functions of index n , respectively. Therefore,

$$a_{-n}(f) = a_n(f), \quad n = 1, 2, \dots, N', \quad (6.1-94)$$

and

$$\theta_{-n}(f) = -\theta_n(f), \quad n = 1, 2, \dots, N'. \quad (6.1-95)$$

Since an odd function passes through the origin, the phase weight associated with element $n = 0$ – which is centered at $x_0 = 0$ – is

$$\theta_0(f) = 0. \quad (6.1-96)$$

Therefore, the complex weight for element $n = 0$ is

$$c_0(f) = a_0(f). \quad (6.1-97)$$

In order to simplify $S(f, f_X)$, first rewrite it as follows:

$$S(f, f_X) = c_0(f) + \sum_{n=1}^{N'} [c_{-n}(f) \exp(+j2\pi f_X x_{-n}) + c_n(f) \exp(+j2\pi f_X x_n)]. \quad (6.1-98)$$

Then, by substituting (6.1-91) through (6.1-93), and (6.1-97) into (6.1-98), we obtain

$$\begin{aligned} S(f, f_X) &= a_0(f) + \sum_{n=1}^{N'} [c_n^*(f) \exp(-j2\pi f_X nd) + c_n(f) \exp(+j2\pi f_X nd)] \\ &= a_0(f) + \sum_{n=1}^{N'} \left\{ [c_n(f) \exp(+j2\pi f_X nd)]^* + [c_n(f) \exp(+j2\pi f_X nd)] \right\}. \end{aligned} \quad (6.1-99)$$

Since $Z^* + Z = 2 \operatorname{Re}\{Z\}$, (6.1-99) reduces to

$$S(f, f_X) = a_0(f) + 2 \sum_{n=1}^{N'} \operatorname{Re}\{c_n(f) \exp(+j2\pi f_X nd)\}, \quad (6.1-100)$$

and by substituting (6.1-6) into (6.1-100), we finally obtain

$$S(f, f_X) = a_0(f) + 2 \sum_{n=1}^{N'} a_n(f) \cos[2\pi f_X nd + \theta_n(f)] \quad (6.1-101)$$

where N' is given by (6.1-84). Equation (6.1-101) is valid only if all the identical elements in the array are equally spaced and the complex weights satisfy the conjugate symmetry property given by (6.1-93).

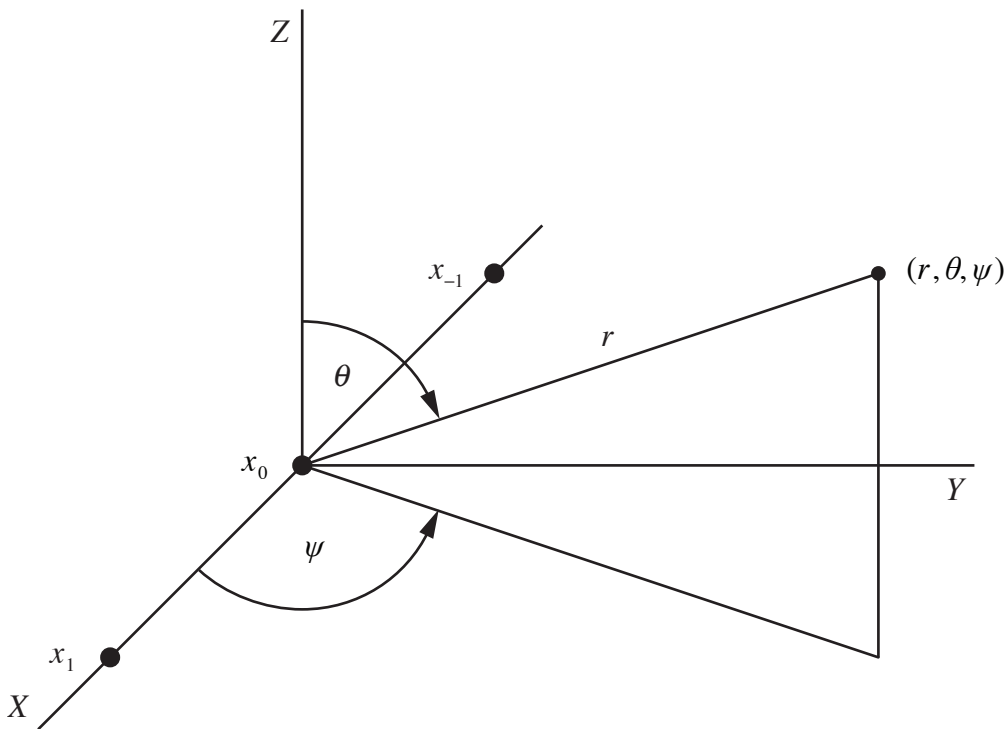


Figure 6.1-8 Linear array of three omnidirectional point-elements lying along the X axis. Also shown is a field point with spherical coordinates (r, θ, ψ) .

Example 6.1-4 Axial Quadrupole

An *axial quadrupole* is a linear array of three identical, equally-spaced, complex-weighted, omnidirectional point-elements where the complex weights satisfy the conjugate symmetry property given by (6.1-93) (see Fig. 6.1-8). Substituting $N = 3$ into (6.1-84) yields $N' = 1$. Since the elements are equally spaced, substituting $N' = 1$ into (6.1-91) yields the following x coordinates of the centers of the three elements:

$$x_{-1} = -d, \quad (6.1-102)$$

$$x_0 = 0, \quad (6.1-103)$$

and

$$x_1 = d \quad (6.1-104)$$

so that the interelement spacing is d meters. Since the complex weights satisfy the conjugate symmetry property given by (6.1-93), substituting $N' = 1$ into (6.1-94) and (6.1-95) yields

$$a_{-1}(f) = a_1(f) \quad (6.1-105)$$

and

$$\theta_{-1}(f) = -\theta_1(f). \quad (6.1-106)$$

For an axial quadrupole,

$$a_0(f) = -2a_1(f). \quad (6.1-107)$$

And since the elements are identical, substituting (6.1-107) and $N'=1$ into (6.1-101), and then substituting the result into (6.1-89) yields

$$D(f, f_X) = 2a_1(f)\mathcal{S}(f)[\cos[2\pi f_X d + \theta_1(f)] - 1] \quad (6.1-108)$$

where $\mathcal{S}(f)$ is the complex, element sensitivity function. Equation (6.1-108) is the *unnormalized*, far-field beam pattern of an axial quadrupole lying along the X axis.

The magnitude of the far-field beam pattern given by (6.1-108) is

$$|D(f, f_X)| = 2|a_1(f)| |\mathcal{S}(f)| |\cos[2\pi f_X d + \theta_1(f)] - 1|, \quad (6.1-109)$$

and since the maximum value of $|\cos[2\pi f_X d + \theta_1(f)] - 1|$ is 2,

$$D_{\max} = 4|a_1(f)| |\mathcal{S}(f)|. \quad (6.1-110)$$

Dividing (6.1-109) by (6.1-110) yields the following expression for the magnitude of the *normalized*, far-field beam pattern of an axial quadrupole lying along the X axis:

$$|D_N(f, f_X)| = 0.5 |\cos[2\pi f_X d + \theta_1(f)] - 1| \quad (6.1-111)$$

If we let $\theta_1(f) = 0$, that is, if only amplitude weighting is done (no phase weighting), then (6.1-111) reduces to

$$|D_N(f, f_X)| = 0.5 |\cos(2\pi f_X d) - 1|. \quad (6.1-112)$$

Since spatial frequency

$$f_X = u/\lambda = \sin\theta \cos\psi/\lambda, \quad (6.1-113)$$

(6.1-112) can also be expressed as

$$|D_N(f, u)| = \frac{1}{2} \left| \cos\left(2\pi \frac{d}{\lambda} u\right) - 1 \right|, \quad (6.1-114)$$

or

$$|D_N(f, \theta, \psi)| = \frac{1}{2} \left| \cos\left(2\pi \frac{d}{\lambda} \sin \theta \cos \psi\right) - 1 \right|. \quad (6.1-115)$$

At broadside where direction cosine $u = 0$, (6.1-114) reduces to $|D_N(f, 0)| = 0$, and by setting $\theta = 90^\circ$ in (6.1-115), we obtain

$$|D_N(f, 90^\circ, \psi)| = \frac{1}{2} \left| \cos\left(2\pi \frac{d}{\lambda} \cos \psi\right) - 1 \right|, \quad (6.1-116)$$

which is the magnitude of the normalized, *horizontal*, far-field beam pattern in the *XY* plane of an axial quadrupole lying along the *X* axis (see Fig. 6.1-9). The far-field beam patterns of both the dipole (see Fig. 6.1-4) and the axial quadrupole have nulls at broadside. ■

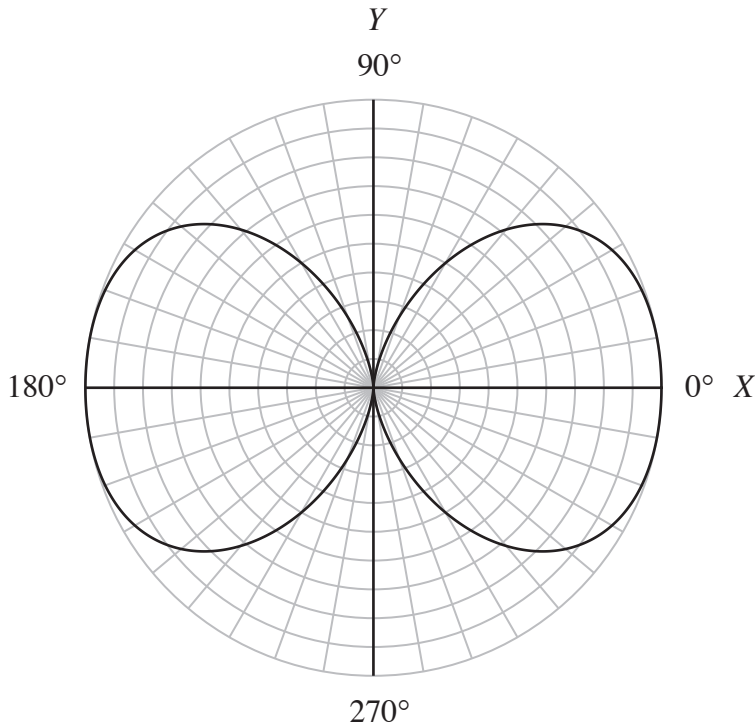


Figure 6.1-9 Polar plot, as a function of the azimuthal (bearing) angle ψ , of the magnitude of the normalized, horizontal, far-field beam pattern of an axial quadrupole lying along the *X* axis given by (6.1-116) for $d/\lambda = 0.5$.

6.2 Common Amplitude Weights and Corresponding Far-Field Beam Patterns

The most common set of amplitude weights are simply sampled values of the continuous amplitude windows already discussed in [Section 2.2](#). For example, consider the following set of equations, where $n = -(N-1)/2, \dots, 0, \dots, (N-1)/2$ and N is odd:

(1) rectangular amplitude weight:

$$a_n(f) = 1 \quad (6.2-1)$$

(2) triangular amplitude weight:

$$a_n(f) = 1 - \frac{|n|}{(N-1)/2} \quad (6.2-2)$$

(3) cosine amplitude weight:

$$a_n(f) = \cos\left(\frac{\pi n}{N-1}\right) \quad (6.2-3)$$

(4) Hanning amplitude weight:

$$a_n(f) = 0.5 + 0.5 \cos\left(\frac{2\pi n}{N-1}\right) \quad (6.2-4)$$

(5) Hamming amplitude weight:

$$a_n(f) = 0.54 + 0.46 \cos\left(\frac{2\pi n}{N-1}\right) \quad (6.2-5)$$

(6) Blackman amplitude weight:

$$a_n(f) = 0.42 + 0.5 \cos\left(\frac{2\pi n}{N-1}\right) + 0.08 \cos\left(\frac{4\pi n}{N-1}\right) \quad (6.2-6)$$

Although the amplitude weight $a_n(f)$ is, in general, a function of frequency, the amplitude weights given by (6.2-1) through (6.2-6) are not functions of frequency, but they are *even* functions of index (element number) n . Amplitude weights, as

well as phase weights, are implemented by using digital signal processing (digital beamforming), as will be discussed in [Section 6.4](#). The process of amplitude weighting an array of elements is also known as amplitude shading or as applying an amplitude window to the array. Note that the amplitude weights given by (6.2-1) through (6.2-6) are also used in frequency spectrum analysis problems as well.

The far-field beam pattern $D(f, f_X)$ of a linear array composed of an odd number N of identical elements lying along the X axis, where each element is a single continuous line source or receiver L meters in length, is given by the Product Theorem [see (6.1-86)]

$$D(f, f_X) = E(f, f_X)S(f, f_X), \quad (6.2-7)$$

where $E(f, f_X)$ is the far-field beam pattern of one of the identical elements in the array, and the array factor $S(f, f_X)$ is given by (6.1-87) for N odd. If the elements are equally spaced and only amplitude weighting is done (no phase weighting), then $S(f, f_X)$ reduces to

$$S(f, f_X) = \sum_{n=-N'}^{N'} a_n(f) \exp(+j2\pi f_X n d), \quad (6.2-8)$$

where

$$N' = (N - 1)/2. \quad (6.2-9)$$

Next we shall show how to obtain closed-form expressions for (6.2-8) for the amplitude weights given by (6.2-1), and (6.2-3) through (6.2-6).

Consider the following set of amplitude weights:

$$a_n(f) = A \cos\left(\frac{b\pi n}{N-1}\right), \quad n = -N', \dots, 0, \dots, N', \quad (6.2-10)$$

where A and b are real constants. Note that the amplitude weights given by (6.2-1), and (6.2-3) through (6.2-6) all involve one or more terms of the form of (6.2-10), where A takes on values of 1, 0.5, 0.54, 0.46, 0.42, and 0.08; and b takes on values of 0, 1, 2, and 4. Since (6.2-10) can be rewritten as

$$a_n(f) = \frac{A}{2} \exp\left(+j\frac{b\pi n}{N-1}\right) + \frac{A}{2} \exp\left(-j\frac{b\pi n}{N-1}\right), \quad (6.2-11)$$

and since

$$\sum_{k=-K}^K \exp(+jk\alpha) = \frac{\sin[(2K+1)\alpha/2]}{\sin(\alpha/2)}, \quad (6.2-12)$$

substituting (6.2-11) into (6.2-8), and using (6.2-12) yields

$$S(f, f_x) = \frac{A}{2} \frac{\sin\left(\pi f_x N d + \frac{b\pi N}{2(N-1)}\right)}{\sin\left(\pi f_x d + \frac{b\pi}{2(N-1)}\right)} + \frac{A}{2} \frac{\sin\left(\pi f_x N d - \frac{b\pi N}{2(N-1)}\right)}{\sin\left(\pi f_x d - \frac{b\pi}{2(N-1)}\right)}$$
(6.2-13)

Because the set of amplitude weights given by (6.2-10) is analogous to the continuous aperture function given by (2.2-23), it is not surprising that (6.2-13) is analogous to (2.2-29).

Equation (6.2-13) is a very important result because it can be used to obtain closed-form expressions for the array factor $S(f, f_x)$ given by (6.2-8) for the rectangular, cosine, Hanning, Hamming, and Blackman amplitude weights. For example, if we let $A = 1$ and $b = 0$, then (6.2-10) reduces to

$$a_n(f) = 1, \quad n = -N', \dots, 0, \dots, N', \quad (6.2-14)$$

which is the set of rectangular amplitude weights given by (6.2-1). And with $A = 1$ and $b = 0$, (6.2-13) reduces to

$$S(f, f_x) = \frac{\sin(\pi f_x N d)}{\sin(\pi f_x d)} \quad (6.2-15)$$

where the normalization factor $S_{\max} = N$ [see (6.1-88)]. Since $a_n(f) > 0 \quad \forall n$ in this case, the array factor has its maximum value at broadside, that is, $S_{\max} = |S(f, 0)| = N$ [see (6.2-8) or use L'Hospital's rule to evaluate (6.2-15) at $f_x = 0$]. In contrast, for the dipole discussed in [Example 6.1-2](#), and the axial quadrupole discussed in [Example 6.1-4](#), the array factor has a null at broadside, that is, $S(f, 0) = 0$. Since spatial frequency

$$f_x = u/\lambda = \sin\theta \cos\psi/\lambda, \quad (6.2-16)$$

(6.2-15) can also be expressed as

$$S(f, u) = \frac{\sin\left(N\pi \frac{d}{\lambda} u\right)}{\sin\left(\pi \frac{d}{\lambda} u\right)}, \quad (6.2-17)$$

or

$$S(f, \theta, \psi) = \frac{\sin\left(N\pi \frac{d}{\lambda} \sin\theta \cos\psi\right)}{\sin\left(\pi \frac{d}{\lambda} \sin\theta \cos\psi\right)}. \quad (6.2-18)$$

As you may have noticed, (6.2-10) and (6.2-13) are not applicable for the set of triangular amplitude weights given by (6.2-2). Therefore, for completeness, the closed-form expression for the array factor $S(f, f_x)$ given by (6.2-8) for the set of triangular amplitude weights is given by

$$S(f, f_x) = \frac{2}{N-1} \frac{\sin^2[\pi f_x (N-1)d/2]}{\sin^2(\pi f_x d)} \quad (6.2-19)$$

where the normalization factor $S_{\max} = (N-1)/2$ [see (6.1-88)]. Since $a_n(f) \geq 0 \forall n$ in this case, the array factor has its maximum value at broadside, that is, $S_{\max} = |S(f, 0)| = (N-1)/2$.

Because the amplitude weights given by (6.2-1) through (6.2-6) are *even* functions of index (element number) n , their array factors are *real, even* functions of spatial frequency f_x (direction cosine u) [e.g., see (6.2-15) and (6.2-19)]. In general, if an amplitude weight is an *even* function of index n , then the corresponding array factor will be a *real, even* function of the appropriate spatial frequency (direction cosine). Similarly, if an amplitude weight is an *odd* function of index n , then the corresponding array factor will be an *imaginary, odd* function of the appropriate spatial frequency (direction cosine).

Example 6.2-1 Application of the Product Theorem

Consider a linear array composed of an odd number N of identical, equally-spaced elements lying along the X axis, where each element is a single continuous line source or receiver L meters in length. If rectangular amplitude weights are used and no phase weighting is done, then the far-field beam pattern of this array can be obtained by substituting (6.2-15) into the Product Theorem given by (6.2-7). Doing so yields

$$D(f, f_x) = E(f, f_x) \frac{\sin(\pi f_x N d)}{\sin(\pi f_x d)}. \quad (6.2-20)$$

If the complex frequency responses (complex aperture functions) of the identical elements are modeled by the continuous rectangular amplitude window, then from [Subsection 2.2.1](#),

$$e(f, x_A) = A_A \operatorname{rect}(x_A/L) \quad (6.2-21)$$

and

$$E(f, f_X) = A_A L \operatorname{sinc}(f_X L), \quad (6.2-22)$$

where

$$\operatorname{sinc}(x) \triangleq \frac{\sin(\pi x)}{\pi x} \quad (6.2-23)$$

and the real, positive constant A_A carries the correct units of $e(f, x_A)$ (see Table 6.1-1). Although A_A is shown here as a constant, as was previously mentioned in Subsection 2.2.1, A_A is, in general, a real, nonnegative function of frequency, that is, $A_A \rightarrow A_A(f)$. Therefore, substituting (6.2-22) into (6.2-20) yields

$$D(f, f_X) = A_A L \operatorname{sinc}(f_X L) \frac{\sin(\pi f_X N d)}{\sin(\pi f_X d)}, \quad (6.2-24)$$

where, at broadside,

$$D(f, 0) = N A_A L. \quad (6.2-25)$$

If the identical elements in the array are omnidirectional point-elements instead, then [see (6.1-14)]

$$e(f, x_A) = \mathcal{S}(f) \delta(x_A) \quad (6.2-26)$$

and [see (6.1-16)]

$$E(f, f_X) = \mathcal{S}(f), \quad (6.2-27)$$

where $\mathcal{S}(f)$ is the complex, element sensitivity function (see Table 6.1-2 and Appendix 6B). Therefore, substituting (6.2-27) into (6.2-20) yields

$$D(f, f_X) = \mathcal{S}(f) \frac{\sin(\pi f_X N d)}{\sin(\pi f_X d)}, \quad (6.2-28)$$

where, at broadside,

$$D(f, 0) = N \mathcal{S}(f). \quad (6.2-29)$$

We shall finish our discussion in this example by investigating what happens to the far-field beam pattern $E(f, f_X)$ given by (6.2-22) and, hence, the far-field beam pattern $D(f, f_X)$ given by (6.2-24), if the length L is small compared to a wavelength. Since

$$\sin \alpha \approx \alpha, \quad \alpha \leq 0.0873 \text{ rad}, \quad (6.2-30)$$

then

$$\sin(\pi f_x L) \approx \pi f_x L \quad (6.2-31)$$

whenever

$$\pi f_x L = \pi u L / \lambda \leq 0.0873. \quad (6.2-32)$$

Setting direction cosine u equal to its maximum positive value of 1 (worst case – harder to satisfy the inequality) yields

$$L / \lambda \leq 0.0278. \quad (6.2-33)$$

Therefore, if (6.2-33) is satisfied, then the approximation given by (6.2-31) is valid and (6.2-22) reduces to

$$E(f, f_x) = A_A L \frac{\sin(\pi f_x L)}{\pi f_x L} \approx A_A L, \quad \frac{L}{\lambda} \leq 0.0278, \quad (6.2-34)$$

and by substituting (6.2-34) into (6.2-20), we obtain

$$D(f, f_x) \approx A_A L \frac{\sin(\pi f_x N d)}{\sin(\pi f_x d)}, \quad \frac{L}{\lambda} \leq 0.0278, \quad (6.2-35)$$

where, at broadside,

$$D(f, 0) \approx N A_A L, \quad L / \lambda \leq 0.0278. \quad (6.2-36)$$

Compare (6.2-35) with (6.2-24) and (6.2-28). Since the far-field beam pattern given by (6.2-34) is not a function of the spherical angles θ and ψ , the identical elements are omnidirectional. In other words, the elements transmit and/or receive equally well in all directions. If we let $L_{\max} = 0.0278\lambda$, then the far-field beam patterns $E(f, f_x)$ and $D(f, f_x)$ given by (6.2-34) and (6.2-35) are valid as long as $L \leq L_{\max}$ (see Table 6.2-1). ■

Table 6.2-1 Values for the Maximum Length $L_{\max} = 0.0278\lambda$ for Three Different Frequencies f . Note that 1 in = 2.54 cm .

c (m/sec)	f (kHz)	λ (m)	L_{\max} (cm)	L_{\max} (in)
1500	0.1	15.0	41.7	16.4
1500	1.0	1.5	4.17	1.64
1500	10.0	0.15	0.417	0.164

In [Example 6.2-1](#), we were able to obtain three different closed-form expressions for the unnormalized, far-field beam pattern $D(f, f_X)$ of a linear array, namely (6.2-24), (6.2-28), and (6.2-35). If a closed-form expression for the far-field beam pattern of a linear array can be derived, then the dimensionless 3-dB beamwidth Δu in direction-cosine space of its beam pattern can be obtained using the procedure outlined in [Example 2.3-3](#). Once Δu has been determined, the 3-dB beamwidths $\Delta\theta$ and $\Delta\psi$ in degrees, of the vertical and horizontal, far-field beam patterns can be obtained by using (2.3-19) and (2.3-25), respectively.

Example 6.2-2 Closed-Form Expression for the Array Factor for Rectangular Amplitude Weights when N is Even

Consider a linear array composed of an *even* number N of identical, equally-spaced, complex-weighted elements lying along the X axis, where each element is a single continuous line source or receiver L meters in length, and the complex weights satisfy the conjugate symmetry property given by (6.1-22). The far-field beam pattern of this array is given by the Product Theorem [see (6.1-10)]

$$D(f, f_X) = E(f, f_X)S(f, f_X), \quad (6.2-37)$$

where [see (6.1-27)]

$$S(f, f_X) = 2 \sum_{n=1}^{N/2} \operatorname{Re}\left\{c_n(f) \exp[+j2\pi f_X(n-0.5)d]\right\}, \quad (6.2-38)$$

or

$$S(f, f_X) = 2 \operatorname{Re}\left\{\exp(-j\pi f_X d) \sum_{n=1}^{N/2} c_n(f) \exp(+j2\pi f_X n d)\right\}. \quad (6.2-39)$$

If rectangular amplitude weights are used and no phase weighting is done, then $c_n(f) = 1 \forall n$ and (6.2-39) reduces to

$$S(f, f_X) = 2 \operatorname{Re}\left\{\exp(-j\pi f_X d) \sum_{n=1}^{N/2} \exp(+j2\pi f_X n d)\right\}. \quad (6.2-40)$$

In order to obtain a closed-form expression for $S(f, f_X)$ as given by (6.2-40), we need to rewrite the summation by letting $m = n - 1$. Doing so yields

$$\sum_{n=1}^{N/2} \exp(+j2\pi f_X n d) = \exp(+j2\pi f_X d) \sum_{m=0}^M \exp(+j2\pi f_X m d) = \exp(+j2\pi f_X d) \sum_{m=0}^M x^m, \quad (6.2-41)$$

where

$$M = \frac{N}{2} - 1 \quad (6.2-42)$$

and

$$x = \exp(+j2\pi f_x d). \quad (6.2-43)$$

Since

$$\sum_{m=0}^M x^m = \frac{x^{M+1} - 1}{x - 1}, \quad x \neq 1, \quad (6.2-44)$$

$$\sum_{n=1}^{N/2} \exp(+j2\pi f_x n d) = \exp(+j\pi f_x d) \exp(+j\pi f_x N d / 2) \frac{\sin(\pi f_x N d / 2)}{\sin(\pi f_x d)}. \quad (6.2-45)$$

Substituting (6.2-45) into (6.2-40) yields the desired result:

$$S(f, f_x) = 2 \cos(\pi f_x N d / 2) \frac{\sin(\pi f_x N d / 2)}{\sin(\pi f_x d)} \quad (6.2-46)$$

where the normalization factor $S_{\max} = N$ [see (6.1-13)]. Note that in this case, $|S(f, 0)| = N$. Compare (6.2-46) for N even with (6.2-15) for N odd. ■

6.3 Dolph-Chebyshev Amplitude Weights

The far-field beam pattern of a linear array of N identical, complex-weighted elements lying along the X axis, where each element is a single continuous line source or receiver L meters in length, is given by the Product Theorem

$$D(f, f_x) = E(f, f_x) S(f, f_x). \quad (6.3-1)$$

If the elements are equally-spaced, the complex weights satisfy the conjugate symmetry property given by (6.1-22) for N even, and (6.1-93) for N odd, and no phase weighting is done [i.e., $\theta_n(f) = 0 \quad \forall n$], then the array factor given by (6.1-28) for N even reduces to

$$S(f, f_x) = 2 \sum_{n=1}^{N/2} a_n(f) \cos[2\pi f_x (n - 0.5)d], \quad (6.3-2)$$

and the array factor given by (6.1-101) for N odd reduces to

$$S(f, f_X) = a_0(f) + 2 \sum_{n=1}^{N'} a_n(f) \cos(2\pi f_X n d), \quad (6.3-3)$$

where

$$N' = (N - 1)/2. \quad (6.3-4)$$

We know from our discussion of linear apertures in [Section 2.2](#) that different amplitude windows yield far-field beam patterns with different sidelobe levels and beamwidths, and as sidelobe levels decrease, beamwidth generally increases. This principle also applies to the far-field beam patterns of amplitude-weighted arrays. However, the Dolph-Chebyshev method of computing amplitude weights makes it possible to *optimize* the array factor $S(f, f_X)$ so that for any specified sidelobe level relative to the level of the mainlobe, the *smallest* possible mainlobe beamwidth for $S(f, f_X)$ is achieved, or for any specified mainlobe beamwidth, the *lowest* possible sidelobe level for $S(f, f_X)$ is achieved. The number of elements N can be either even or odd, and the resulting Dolph-Chebyshev amplitude weights are *even* functions of element number n . Although the sidelobe level and mainlobe beamwidth of $S(f, f_X)$ can be optimized, the overall far-field beam pattern of the array $D(f, f_X)$ is still equal to $S(f, f_X)$ multiplied by the far-field beam pattern $E(f, f_X)$ of one of the identical elements in the array. The far-field beam pattern $E(f, f_X)$ has its own sidelobe levels and mainlobe beamwidth, unless it is omnidirectional. The one disadvantage of the Dolph-Chebyshev method is that *all* of the sidelobes of $S(f, f_X)$ are at the *same* level – they do not fall off in value.

We begin our discussion of the Dolph-Chebyshev method of computing amplitude weights by letting

$$\alpha = \pi f_X d. \quad (6.3-5)$$

Substituting (6.3-5) into (6.3-2) and (6.3-3) yields

$$\begin{aligned} S(f, f_X) &= 2 \sum_{n=1}^{N/2} a_n(f) \cos[(2n-1)\alpha] \\ &= 2a_1(f)\cos(\alpha) + 2a_2(f)\cos(3\alpha) + \dots + 2a_{N/2}(f)\cos[(N-1)\alpha] \end{aligned} \quad (6.3-6)$$

and

$$\begin{aligned} S(f, f_X) &= a_0(f) + 2 \sum_{n=1}^{N'} a_n(f) \cos(2n\alpha) \\ &= a_0(f) + 2a_1(f)\cos(2\alpha) + 2a_2(f)\cos(4\alpha) + \dots + 2a_{N'}(f)\cos(2N'\alpha), \end{aligned} \quad (6.3-7)$$

respectively. Since the m th-degree Chebyshev polynomial is given by

$$T_m(x) = \begin{cases} \cos[m \cos^{-1} x], & |x| \leq 1 \\ \cosh[m \cosh^{-1} x], & x \geq 1 \\ (-1)^m \cosh[m \cosh^{-1}(-x)], & x \leq -1 \end{cases} \quad (6.3-8)$$

if we also let [see (6.3-5)]

$$\alpha = \cos^{-1} x \quad (6.3-9)$$

so that

$$x = \cos \alpha, \quad (6.3-10)$$

then

$$T_m(x) = \cos(m\alpha), \quad |x| \leq 1. \quad (6.3-11)$$

By comparing (6.3-11) with (6.3-6) and (6.3-7), it can be seen that $S(f, f_x)$ can be expressed as a sum of Chebyshev polynomials. The degree of the polynomial $S(f, f_x)$, which is called the *array polynomial*, is

$$i = N - 1 \quad (6.3-12)$$

or one less than the total number of elements in the array. Because the Dolph-Chebyshev method depends on certain properties of Chebyshev polynomials, we must digress for a moment to discuss these properties before continuing further.

All Chebyshev polynomials possess the following two important properties:

(1) $T_m(x)$ has unit-magnitude maxima and minima that occur alternately at

$$x_k = \cos(k\pi/m), \quad k = 1, 2, \dots, m-1, \quad (6.3-13)$$

where $-1 < x_k < 1$ and $|T_m(x_k)| = 1$. Therefore, Chebyshev polynomials have an “equal ripple” characteristic in the interval $-1 < x < 1$.

(2) At $x = \pm 1$, $|T_m(\pm 1)| = 1$. However, $|T_m(x)| > 1$ for $|x| > 1$ and

$$\left| \frac{d}{dx} T_m(x) \right|_{x=\pm 1} = m^2. \quad (6.3-14)$$

Chebyshev polynomials possess additional properties, but they are not pertinent to the present problem.

In the Dolph-Chebyshev method, the magnitude of the level of the mainlobe of $S(f, f_X)$ corresponds to the value of $T_i(x_0)$, where i is the degree of the array polynomial given by (6.3-12) and $x_0 > 1$. The magnitude of the level of the sidelobes of $S(f, f_X)$ is numerically equal to the absolute value of the interior maxima and minima, that is, 1. Note that it is the “equal ripple” characteristic of Chebyshev polynomials, as discussed in property (1), that is responsible for generating sidelobes all at the same level in the Dolph-Chebyshev method of computing amplitude weights. Therefore, the ratio

$$\frac{|\text{mainlobe level}|}{|\text{sidelobe level}|} = |\text{mainlobe level}| = T_i(x_0) = r > 1, \quad (6.3-15)$$

is used to determine the value of x_0 , that is, we solve for x_0 using the equation $T_i(x_0) = r$. But in order to compute a value for x_0 , we need a value for r .

A value for the ratio r is determined as follows: If you want the magnitude of the level of the mainlobe to be R dB above the magnitude of the level of the sidelobes, then

$$20 \log_{10} r = R \text{ dB}, \quad (6.3-16)$$

from which we obtain

$$r = 10^{R/20} \quad (6.3-17)$$

Since the ratio $r > 1$, in order for $T_i(x_0)$ to be greater than 1, x_0 needs to be greater than 1 (see Property 2). Therefore, by referring to (6.3-8),

$$T_i(x_0) = \cosh[i \cosh^{-1} x_0] = r, \quad x_0 > 1. \quad (6.3-18)$$

Solving for x_0 yields

$$x_0 = \cosh\left(\frac{1}{i} \cosh^{-1} r\right), \quad r > 1 \quad (6.3-19)$$

where i is given by (6.3-12) and r is given by (6.3-17). Now that we know how to compute a value for x_0 , we can use it to compute the amplitude weights.

If the total number of elements N is *even*, then the Dolph-Chebyshev

amplitude weights are given by¹

$$\boxed{a_n(f) = \sum_{j=n}^{N/2} [(-1)^{(N/2)-j}] \frac{N-1}{N+2(j-1)} \binom{(N/2)+j-1}{2j-1} \binom{2j-1}{j-n} x_0^{2j-1}, \quad n=1, 2, \dots, \frac{N}{2}} \quad (6.3-20)$$

where

$$\binom{a}{b} = \frac{a!}{b!(a-b)!} \quad (6.3-21)$$

is the binomial coefficient, x_0 is given by (6.3-19), and

$$a_{-n}(f) = a_n(f), \quad n=1, 2, \dots, N/2. \quad (6.3-22)$$

If the total number of elements N is *odd*, then the Dolph-Chebyshev amplitude weights are given by¹

$$\boxed{a_n(f) = \sum_{j=n}^{N'} [(-1)^{N'-j}] \frac{N'}{N'+j} \binom{N'+j}{2j} \binom{2j}{j-n} x_0^{2j}, \quad n=0, 1, \dots, N'} \quad (6.3-23)$$

where N' is given by (6.3-4),

$$\binom{a}{b} = \frac{a!}{b!(a-b)!} \quad (6.3-24)$$

is the binomial coefficient, x_0 is given by (6.3-19), and

$$a_{-n}(f) = a_n(f), \quad n=1, 2, \dots, N'. \quad (6.3-25)$$

In both cases, after the amplitude weights have been computed, they can be normalized by dividing each amplitude weight by the largest value.

Next we shall derive an equation for the 3-dB beamwidth $\Delta\psi$ of the horizontal, angular profile of the array factor $S(f, f_X)$. Recall that $S(f, f_X)$ is dimensionless – it is not a far-field beam pattern by itself since $D(f, f_X) = E(f, f_X)S(f, f_X)$. Since the right-hand sides of (6.3-5) and (6.3-9)

¹ R. S. Elliott, *Antenna Theory and Design*, Prentice-Hall, Englewood Cliffs, NJ, 1981, pg. 147.

must be equal,

$$\pi f_x d = \pi \frac{d}{\lambda} u = \cos^{-1} x, \quad (6.3-26)$$

or

$$u = \sin \theta \cos \psi = \frac{\lambda}{\pi d} \cos^{-1} x. \quad (6.3-27)$$

Also, since the linear array lies along the X axis, the horizontal, angular profile of $S(f, f_x)$ lies in the XY plane (see [Example 2.3-2](#)). In the XY plane, $u = \cos \psi$ since $\theta = 90^\circ$. If we let

$$u_+ = \cos \psi_+ > 0, \quad \theta_+ = 90^\circ, \quad (6.3-28)$$

then from (6.3-27),

$$u_+ = \cos \psi_+ = \frac{\lambda}{\pi d} \cos^{-1} x_+, \quad (6.3-29)$$

or

$$\psi_+ = \cos^{-1} \left(\frac{\lambda}{\pi d} \cos^{-1} x_+ \right), \quad (6.3-30)$$

where x_+ is the value of x that corresponds to the bearing angle ψ_+ to a 3-dB down point.

In order to evaluate $\cos^{-1} x_+$ in (6.3-30), it is required that $|x_+| \leq 1$. Since the magnitude of the level of the mainlobe is equal to r [see (6.3-15)], the magnitude of the 3-dB down-point is $\sqrt{2} r / 2$. However, since $\sqrt{2} r / 2 > 1$ and $|T_i(x)| > 1$ only if $|x| > 1$, x_+ has to be scaled by x_0 so that $x = x_0 x_+ > 1$. Therefore, solving for x_+ from [see (6.3-8) for $x \geq 1$]

$$T_i(x_0 x_+) = \cosh[i \cosh^{-1}(x_0 x_+)] = \sqrt{2} r / 2 \quad (6.3-31)$$

yields

$$x_+ = \frac{1}{x_0} \cosh \left(\frac{1}{i} \cosh^{-1} \left(\sqrt{2} r / 2 \right) \right), \quad r > \sqrt{2} \quad (6.3-32)$$

where i is given by (6.3-12), r is given by (6.3-17), and x_0 is given by (6.3-19). And since (see [Example 2.3-2](#)),

$$\Delta \psi = 180^\circ - 2\psi_+, \quad (6.3-33)$$

substituting (6.3-30) into (6.3-33) yields

$$\Delta\psi = 180^\circ - 2 \cos^{-1} \left(\frac{\lambda}{\pi d} \cos^{-1} x_+ \right), \quad \left| \frac{\lambda}{\pi d} \cos^{-1} x_+ \right| \leq 1 \quad (6.3-34)$$

which is the 3-dB beamwidth in degrees of the horizontal, angular profile of the array factor $S(f, f_X)$ in the XY plane, where x_+ is given by (6.3-32). Note that $\cos^{-1} x_+$ must be expressed in radians.

Example 6.3-1

Consider a linear array of 7 identical, equally-spaced elements lying along the X axis, where each element is a single continuous line source or receiver L meters in length. The interelement spacing $d = \lambda/2$ meters. Later, in [Section 6.5](#), we shall show that if $d < \lambda/2$, then grating lobes (extraneous mainlobes) can be avoided for all possible directions of beam steering. Find the set of *normalized*, Dolph-Chebyshev amplitude weights so that the magnitude of the level of the mainlobe of the array factor $S(f, f_X)$ is 30 dB above the magnitude of the level of its sidelobes. Also, compute the 3-dB beamwidth in degrees of the horizontal, angular profile of $S(f, f_X)$ in the XY plane.

Since $N = 7$ [see (6.3-12)],

$$i = 6, \quad (6.3-35)$$

and since $R = 30$ dB [see (6.3-17)],

$$r = 31.6227766. \quad (6.3-36)$$

Substituting (6.3-35) and (6.3-36) into (6.3-19) yields

$$x_0 = 1.2484890. \quad (6.3-37)$$

Since $N = 7$ [see (6.3-4)],

$$N' = 3. \quad (6.3-38)$$

And finally, substituting (6.3-37) and (6.3-38) into (6.3-23), *normalizing* the Dolph-Chebyshev amplitude weights, and using (6.3-25) yields

$$a_0(f) = 1 \quad (6.3-39)$$

and

$$a_{-1}(f) = a_1(f) = 0.873814 \quad (6.3-40)$$

$$a_{-2}(f) = a_2(f) = 0.568269 \quad (6.3-41)$$

$$a_{-3}(f) = a_3(f) = 0.264225 \quad (6.3-42)$$

We shall compute the 3-dB beamwidth next. Substituting (6.3-35) through (6.3-37) into (6.3-32) yields

$$x_+ = 0.9670442 , \quad (6.3-43)$$

and by substituting (6.3-43) and $d = \lambda/2$ into (6.3-34), we obtain

$$\Delta\psi = 18.9^\circ , \quad (6.3-44)$$

which is the 3-dB beamwidth of the horizontal, angular profile of the array factor $S(f, f_X)$ in the XY plane for $N = 7$, $d = \lambda/2$, and $R = 30$ dB.

In order to verify that the magnitude of the level of the mainlobe of $S(f, f_X)$ is 30 dB above the magnitude of the level of its sidelobes, we shall plot $|S_N(f, u)|$ in decibels versus direction cosine u . But first, we need to derive an equation for the normalized array factor $S_N(f, f_X)$, where $S(f, f_X)$ is given by (6.3-3).

The normalized array factor $S_N(f, f_X)$ is defined as follows:

$$S_N(f, f_X) \triangleq S(f, f_X)/S_{\max} \quad (6.3-45)$$

where $S_{\max} = \max|S(f, f_X)|$ is the normalization factor. Since the Dolph-Chebyshev amplitude weights are *positive* in value for all n , the maximum value of the magnitude of $S(f, f_X)$ given by (6.3-3) occurs at broadside, that is, when spatial frequency $f_X = 0$. Therefore, the normalization factor $S_{\max} = |S(f, 0)|$. Evaluating (6.3-3) at $f_X = 0$ yields

$$S_{\max} = a_0(f) + 2 \sum_{n=1}^{N'} a_n(f) , \quad (6.3-46)$$

and by substituting (6.3-3) and (6.3-46) into (6.3-45), we obtain

$$S_N(f, f_X) = \frac{a_0(f) + 2 \sum_{n=1}^{N'} a_n(f) \cos(2\pi f_X n d)}{a_0(f) + 2 \sum_{n=1}^{N'} a_n(f)} . \quad (6.3-47)$$

The normalization factor given by (6.1-88) for N odd can also be used.

Since

$$f_X = u/\lambda = \sin\theta \cos\psi/\lambda , \quad (6.3-48)$$

substituting (6.3-48) into (6.3-47) yields

$$S_N(f, u) = \frac{a_0(f) + 2 \sum_{n=1}^{N'} a_n(f) \cos\left(2n\pi \frac{d}{\lambda} u\right)}{a_0(f) + 2 \sum_{n=1}^{N'} a_n(f)}. \quad (6.3-49)$$

And since $d = \lambda/2$ in this example, (6.3-49) reduces to

$$S_N(f, u) = \frac{a_0(f) + 2 \sum_{n=1}^{N'} a_n(f) \cos(n\pi u)}{a_0(f) + 2 \sum_{n=1}^{N'} a_n(f)}. \quad (6.3-50)$$

[Figure 6.3-1](#) is a plot of the magnitude of (6.3-50) in decibels versus direction cosine u for $N' = 3$ and the set of Dolph-Chebyshev amplitude weights given by (6.3-39) through (6.3-42). As can be seen from [Fig. 6.3-1](#), the level of the mainlobe is 30 dB above the level of the sidelobes. ■

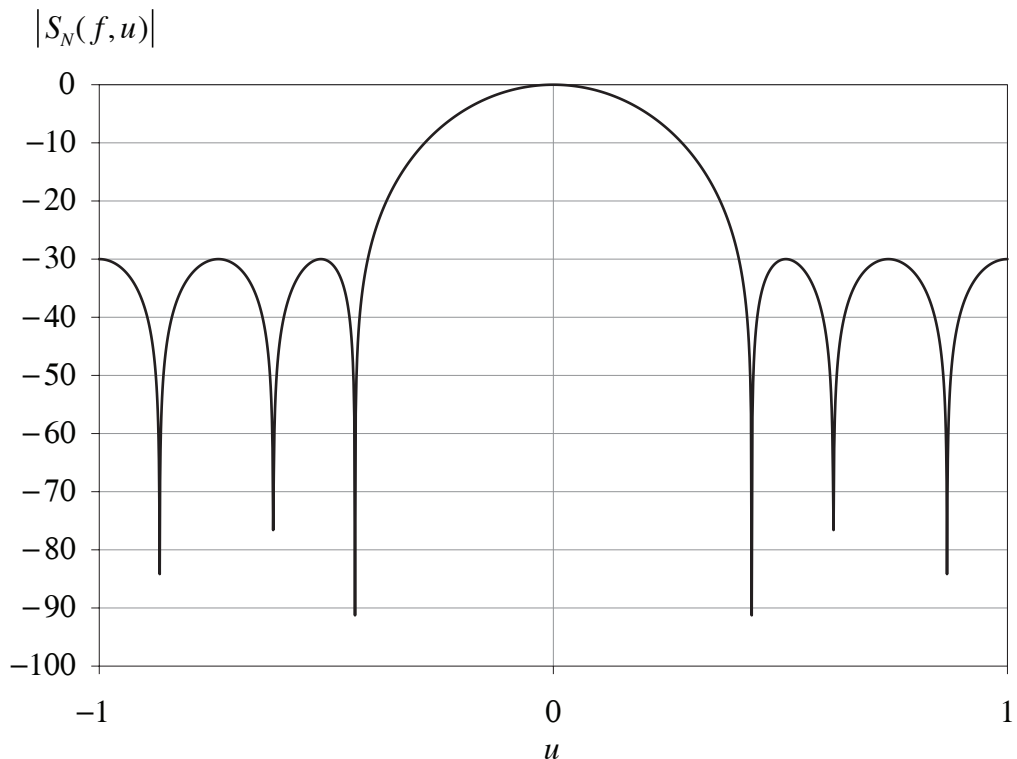


Figure 6.3-1 Plot of the magnitude of (6.3-50) in decibels versus direction cosine u for $N' = 3$ and the set of Dolph-Chebyshev amplitude weights given by (6.3-39) through (6.3-42).

6.4 The Phased Array – Beam Steering

Consider a linear array composed of an odd number N of identical, unevenly-spaced, complex-weighted, omnidirectional point-elements lying along the X axis. From the Product Theorem for an odd number of elements, the far-field beam pattern of this array is given by [see (6.1-89)]

$$D(f, f_X) = \mathcal{S}(f) S(f, f_X), \quad (6.4-1)$$

where $\mathcal{S}(f)$ is the complex, element sensitivity function (see [Table 6.1-2](#) and [Appendix 6B](#)),

$$S(f, f_X) = \sum_{n=-N'}^{N'} c_n(f) \exp(+j2\pi f_X x_n), \quad (6.4-2)$$

$$c_n(f) = a_n(f) \exp[+j\theta_n(f)], \quad (6.4-3)$$

and

$$N' = (N - 1)/2. \quad (6.4-4)$$

Let $D(f, f_X)$ be the far-field beam pattern of the array when it is only amplitude weighted (i.e., $\theta_n(f) = 0 \quad \forall n$), and let $D'(f, f_X)$ be the far-field beam pattern of the array when it is complex weighted. Therefore,

$$D(f, f_X) = \mathcal{S}(f) \sum_{n=-N'}^{N'} a_n(f) \exp(+j2\pi f_X x_n) \quad (6.4-5)$$

and

$$D'(f, f_X) = \mathcal{S}(f) \sum_{n=-N'}^{N'} a_n(f) \exp\{+j[2\pi f_X x_n + \theta_n(f)]\}. \quad (6.4-6)$$

We already know from linear aperture theory that in order to do beam steering, there must be a linear phase response along the length of the aperture (see [Section 2.4](#)). A set of linear phase weights that will produce a linear phase response along the length of the linear array under discussion is given by

$\theta_n(f) = -2\pi f'_X x_n, \quad n = -N', \dots, 0, \dots, N'$

(6.4-7)

where

$f'_X = u'/\lambda = \sin \theta' \cos \psi' / \lambda$

(6.4-8)

If the elements are *equally spaced*, then $x_n = nd$ [see (6.1-91)]. Compare (6.4-7)

and (6.4-8) with (2.4-4) through (2.4-7). If (6.4-7) is substituted into (6.4-6), then

$$D'(f, f_x) = \mathcal{S}(f) \sum_{n=-N'}^{N'} a_n(f) \exp[+j2\pi(f_x - f'_x)x_n], \quad (6.4-9)$$

and by comparing (6.4-9) with (6.4-5),

$$D'(f, f_x) = D(f, f_x - f'_x). \quad (6.4-10)$$

Since spatial frequency

$$f_x = u/\lambda = \sin\theta \cos\psi/\lambda, \quad (6.4-11)$$

(6.4-10) can also be expressed as

$$D'(f, u) = D(f, u - u'). \quad (6.4-12)$$

Equation (6.4-12) indicates that a set of linear phase weights applied along the length of the array will steer the far-field beam pattern $D(f, u)$ of a set of amplitude weights in the direction $u = u'$ in direction-cosine space, which is equivalent to steering (tilting) the beam pattern to $\theta = \theta'$ and $\psi = \psi'$ [see (6.4-8)]. Equal spacing of the elements is *not* required in order to do beam steering. Equation (6.4-12) also indicates that the far-field beam pattern $D'(f, u)$ is simply a translated or shifted version of $D(f, u)$ along the u axis, implying that the shape and beamwidth of the mainlobe of the beam pattern remain unchanged. However, recall from linear aperture theory, that when a beam pattern is steered, the shape and beamwidth of the mainlobe of the beam pattern do change when the magnitude of the beam pattern is plotted as a function of the spherical angles θ and ψ (see [Section 2.5](#)).

It is also important to note that a phase weight $\theta_n(f)$ in radians is equivalent to a *time delay* τ'_n in seconds, that is,

$$\theta_n(f) \triangleq -2\pi f \tau'_n, \quad (6.4-13)$$

or

$$\tau'_n = -\theta_n(f)/(2\pi f). \quad (6.4-14)$$

Substituting (6.4-7) and (6.4-8) into (6.4-14) yields

$$\boxed{\tau'_n = \frac{u'}{c} x_n, \quad n = -N', \dots, 0, \dots, N'} \quad (6.4-15)$$

where $c = f\lambda$.

$$c_n(f) = a_n \exp[+j\theta_n(f)] = a_n \exp(-j2\pi f \tau'_n)$$

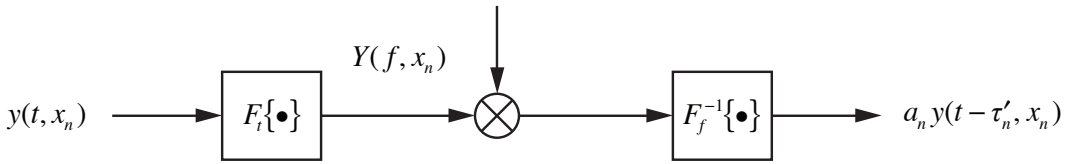


Figure 6.4-1 Beamforming. Implementing a complex weight (amplitude and phase weights) using forward and inverse Fourier transforms.

Figure 6.4-1 illustrates how to implement the complex weight

$$c_n(f) = a_n \exp[+j\theta_n(f)] = a_n \exp(-j2\pi f \tau'_n) \quad (6.4-16)$$

using forward and inverse Fourier transforms. This procedure is referred to as *beamforming*. Note that the amplitude weight a_n is *not* a function of frequency. In Fig. 6.4-1, $y(t, x_n)$ is the output electrical signal from element n in a linear array. The complex weight $c_n(f)$ is just a complex number in a computer program. The expression $F_t\{\bullet\}$ represents a forward Fourier transform with respect to time t , and $F_f^{-1}\{\bullet\}$ represents an inverse Fourier transform with respect to frequency f . In practical applications, the forward and inverse Fourier transforms are computed using forward and inverse *discrete Fourier transforms* (DFTs), which can be evaluated very quickly by using forward and inverse *fast-Fourier-transform* (FFT) algorithms. This is known as *digital beamforming* or *FFT beamforming*. Since the phase weight $\theta_n(f)$ is a function of frequency f , an appropriate phase weight must be applied to *each* frequency component contained in the complex frequency spectrum $Y(f, x_n)$ shown in Fig. 6.4-1 in order to produce the correct time delay τ'_n . This must be done at each element in a linear array.

Example 6.4-1 Steering the Null of a Dipole

The magnitude of the normalized, far-field beam pattern of a dipole lying along the X axis is given by (see Example 6.1-2)

$$|D_N(f, f_X)| = |\sin[\pi f_X d + \theta_l(f)]|. \quad (6.4-17)$$

Since $N = 2$ (an even number) for a dipole, (6.4-7) cannot be used for beam steering. However, all we need to do is to find the equation for the phase weight $\theta_l(f)$ that will generate the factor $f_X - f'_X$ on the right-hand side of (6.4-17).

Therefore, if we let

$$\theta_1(f) = -\pi f'_x d, \quad (6.4-18)$$

then substituting (6.4-18) into (6.4-17) yields

$$|D_N(f, f_x)| = |\sin[\pi(f_x - f'_x)d]|, \quad (6.4-19)$$

where

$$f'_x = u'/\lambda = \sin\theta' \cos\psi'/\lambda. \quad (6.4-20)$$

For completeness, the phase weight at element $n = -1$ is [see (6.1-46)]

$$\theta_{-1}(f) = -\theta_1(f) = \pi f'_x d. \quad (6.4-21)$$

Since spatial frequency

$$f_x = u/\lambda = \sin\theta \cos\psi/\lambda, \quad (6.4-22)$$

(6.4-19) can also be expressed as

$$|D_N(f, u)| = \left| \sin \left[\pi \frac{d}{\lambda} (u - u') \right] \right|, \quad (6.4-23)$$

or

$$|D_N(f, \theta, \psi)| = \left| \sin \left[\pi \frac{d}{\lambda} (\sin\theta \cos\psi - \sin\theta' \cos\psi') \right] \right|. \quad (6.4-24)$$

Setting $\theta = 90^\circ$ and $\theta' = 90^\circ$ in (6.4-24) yields

$$|D_N(f, 90^\circ, \psi)| = \left| \sin \left[\pi \frac{d}{\lambda} (\cos\psi - \cos\psi') \right] \right|, \quad \theta' = 90^\circ, \quad (6.4-25)$$

which is the magnitude of the normalized, *horizontal*, far-field beam pattern in the XY plane of a dipole lying along the X axis, steered to bearing angle ψ' (see Fig. 6.4-2).

Let us end our discussion in this example by deriving the equivalent set of time delays required to steer the far-field beam pattern of a dipole. We cannot use τ'_n given by (6.4-15) because (6.4-15) is only applicable for N odd. However, we can use the general expression for τ'_n given by (6.4-14). Therefore, substituting (6.4-18), (6.4-20), (6.4-21), and $c = f\lambda$ into (6.4-14) yields

$$\tau'_1 = \frac{u' d}{c} \frac{d}{2} \quad (6.4-26)$$

and

$$\tau'_{-1} = -\frac{u' d}{c} \frac{d}{2} \quad (6.4-27)$$

where $u' = \sin \theta' \cos \psi'$. ■

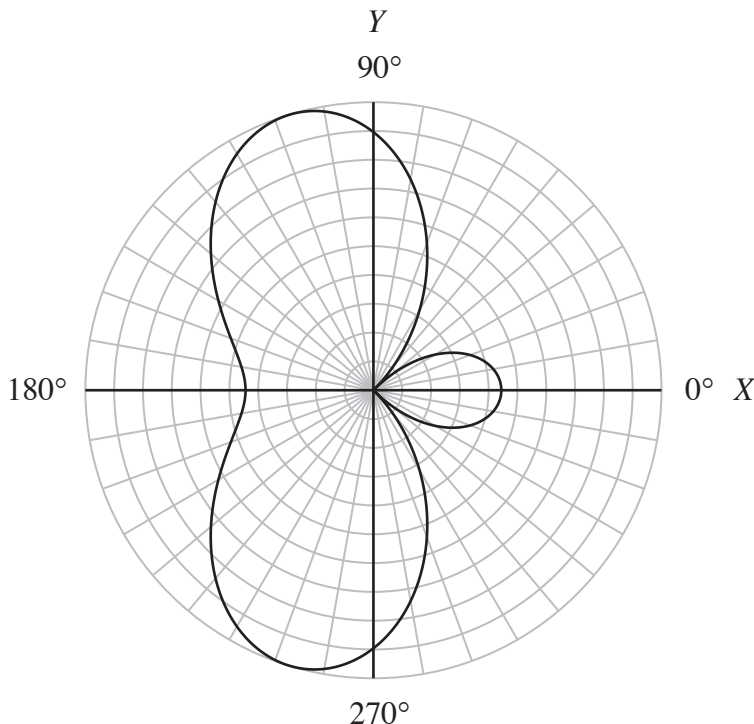


Figure 6.4-2 Polar plot, as a function of the azimuthal (bearing) angle ψ , of the magnitude of the normalized, horizontal, far-field beam pattern of a dipole lying along the X axis given by (6.4-25) for $d/\lambda = 0.5$ and beam-steer angle $\psi' = 45^\circ$.

6.5 Far-Field Beam Patterns and the Spatial Discrete Fourier Transform

In this section we shall show that the far-field beam pattern of a linear array composed of an odd number N of identical, equally-spaced, complex-weighted, omnidirectional point-elements lying along the X axis can be computed using a *spatial* discrete Fourier transform. The far-field beam pattern of the aforementioned array can be obtained by substituting (6.1-87) and (6.1-91)

into (6.1-89). Doing so yields

$$D(f, f_X) = \mathcal{S}(f) \sum_{n=-N'}^{N'} c_n(f) \exp(+j2\pi f_X n d), \quad (6.5-1)$$

where $\mathcal{S}(f)$ is the complex, element sensitivity function (see [Table 6.1-2](#) and [Appendix 6B](#)),

$$c_n(f) = a_n(f) \exp[+j\theta_n(f)], \quad (6.5-2)$$

and

$$N' = (N - 1)/2. \quad (6.5-3)$$

According to (6.5-1), $D(f, f_X)$ is evaluated at continuous values of spatial frequency f_X . A more efficient way to compute $D(f, f_X)$ is to evaluate it at the following set of *discrete* values of f_X :

$$f_X = m \Delta f_X, \quad m = -N'', \dots, 0, \dots, N'', \quad (6.5-4)$$

where

$$\Delta f_X = \frac{1}{(N + Z)d} \leq \frac{1}{Nd} \quad (6.5-5)$$

is the spatial-frequency spacing with units of cycles per meter, Z is a *positive integer* ($Z \geq 0$), d is the interelement spacing in meters, and

$$N'' = \begin{cases} (N + Z)/2, & N + Z \text{ even} \\ (N + Z - 1)/2, & N + Z \text{ odd.} \end{cases} \quad (6.5-6)$$

The ratio $(N + Z)/2$ is referred to as the *folding-bin* whether $N + Z$ is even or odd. Substituting (6.5-4) and (6.5-5) into (6.5-1) yields

$$D(f, m) = \mathcal{S}(f) \sum_{n=-N'}^{N'} c_n(f) W_{N+Z}^{mn}, \quad m = -N'', \dots, 0, \dots, N'' \quad (6.5-7)$$

where the summation on the right-hand side of (6.5-7) is the *spatial discrete Fourier transform* (DFT) of the set of N complex weights $c_n(f)$, and

$$W_{N+Z} = \exp\left(+j \frac{2\pi}{N+Z}\right). \quad (6.5-8)$$

Several comments are in order regarding (6.5-7). First, the index m is referred to as the DFT *bin number*. Evaluating the far-field beam pattern $D(f, m)$ at bin number m corresponds to evaluating the beam pattern at spatial frequency $f_x = m\Delta f_x$. Second, when the integer $Z = 0$, the spatial-frequency spacing (bin spacing) Δf_x is equal to the *maximum* allowed value $1/(Nd)$ [see (6.5-5)], which is the spatial analog of the maximum allowed value of frequency spacing (bin spacing) in hertz in order to avoid aliasing when performing a time-domain DFT. Choosing $Z > 0$ decreases Δf_x and increases N'' . Increasing N'' means that $D(f, m)$ is evaluated at more bins yielding a more smooth curve for plotting purposes. For example, if we want to evaluate $D(f, m)$ at twice as many bins by reducing the bin spacing Δf_x by a factor of two, then set $Z = N$ so that $N + Z = 2N$. This is equivalent to adding $Z = N$ zeros to the original data sequence so that $N + Z = 2N$. Choosing $Z > 0$ is referred to as “padding-with-zeros”. Third, since the spatial DFT is *periodic* with *period* $N + Z$, the far-field beam pattern given by (6.5-7) is *periodic* with *period* $N + Z$, that is,

$$D(f, m + N + Z) = D(f, m). \quad (6.5-9)$$

It is the equal spacing of the elements that is responsible for the periodicity. The periodicity of the DFT is the reason why the range of values for bin number m need only cover one period, as shown in (6.5-7). The reason that negative as well as positive values for bin number m are used is to cover the entire visible region, as shall be discussed later. The fourth and final comment is that a DFT can be evaluated very quickly by using a *fast-Fourier-transform* (FFT) algorithm. Therefore, the far-field beam pattern $D(f, m)$ given by (6.5-7) can be evaluated by using either a DFT or a FFT algorithm. See [Appendix 6E](#) for an equation analogous to (6.5-7) for the case when the number of elements N is even.

Most commonly available FFT algorithms assume that the total number of data points to be processed is equal to an integer power of two, that is,

$$N = 2^b, \quad (6.5-10)$$

where b is a nonzero, positive integer. If N does not satisfy (6.5-10), then simply pick a value for Z so that $N + Z = 2^b$. Since in this section the number of elements N and, hence, complex weights is odd, Z must also be odd in order for $N + Z$ to be equal to an integer power of two, which is an even number. For example, if $N = 7$ and $Z = 9$, then $N + Z = 16 = 2^4$. It is very important to remember that even if $N + Z \neq 2^b$ so that a FFT algorithm cannot be used to evaluate the DFT in (6.5-7), (6.5-7) can still be used to compute the far-field beam pattern $D(f, m)$.

In order to relate a bin number to values of the spherical angles θ and ψ , we first need to derive a relationship between bin number m and the

corresponding value of direction cosine u_m . Since [see (6.5-4)]

$$f_x = \frac{u}{\lambda} = m \Delta f_x, \quad m = -N'', \dots, 0, \dots, N'', \quad (6.5-11)$$

solving for direction cosine u yields

$$u = u_m = m \lambda \Delta f_x, \quad m = -N'', \dots, 0, \dots, N'', \quad (6.5-12)$$

and by substituting (6.5-5) into (6.5-12), we obtain

$$u_m = \frac{m}{N+Z} \frac{\lambda}{d}, \quad m = -N'', \dots, 0, \dots, N'' \quad (6.5-13)$$

where

$$u_m = \sin \theta_m \cos \psi_m \quad (6.5-14)$$

and N'' is given by (6.5-6). If we restrict ourselves to the vertical beam pattern in the XZ plane, then $u_m = \sin \theta_m$ when $\psi_m = 0^\circ$, and $u_m = -\sin \theta_m$ when $\psi_m = 180^\circ$. Similarly, if we restrict ourselves to the horizontal beam pattern in the XY plane, then $u_m = \cos \psi_m$ since $\theta_m = 90^\circ$. Also, since the visible region corresponds to $-1 \leq u_m \leq 1$, and since u_m will take on negative values only for negative values of m , it is important to evaluate the far-field beam pattern given by (6.5-7) at negative and positive bin numbers m .

If we let δu be the direction-cosine bin spacing, then by using (6.5-13)

$$\delta u = u_m - u_{m-1} = \frac{1}{N+Z} \frac{\lambda}{d}. \quad (6.5-15)$$

Solving for Z from (6.5-15) yields

$$Z = \frac{1}{\delta u} \frac{\lambda}{d} - N \quad (6.5-16)$$

Equation (6.5-16) is used to solve for the value of Z that is required in order to obtain a desired direction-cosine bin spacing δu .

The *normalized*, far-field beam pattern $D_N(f, m)$ is given by

$$D_N(f, m) = D(f, m) / D_{\max}, \quad (6.5-17)$$

where $D(f, m)$ is the unnormalized, far-field beam pattern given by (6.5-7), and

if $a_n(f) > 0 \quad \forall n$, then

$$D_{\max} = \max |D(f, m)| = |\mathcal{S}(f)| \sum_{n=-N'}^{N'} a_n(f) \quad (6.5-18)$$

is the normalization factor [use the procedure in [Appendix 6A](#) for N odd to obtain (6.5-18)]. Therefore, dividing the magnitude of (6.5-7) by (6.5-18) yields

$$\left| D_N(f, m) \right| = \frac{\left| \sum_{n=-N'}^{N'} c_n(f) W_{N+Z}^{mn} \right|}{\sum_{n=-N'}^{N'} a_n(f)}, \quad m = -N'', \dots, 0, \dots, N'' \quad (6.5-19)$$

[Figure 6.5-1](#) is a plot of the magnitudes of the normalized, far-field beam patterns of the rectangular, triangular, and cosine amplitude weights given by (6.2-1) through (6.2-3). Compare [Fig. 6.5-1](#) with [Fig. 2.2-9](#). [Figure 6.5-2](#) is a plot of the magnitudes of the normalized, far-field beam patterns of the Hanning, Hamming, and Blackman amplitude weights given by (6.2-4) through (6.2-6). Compare [Fig. 6.5-2](#) with [Fig. 2.2-11](#). [Figures 6.5-1](#) and [6.5-2](#) were obtained by evaluating (6.5-19) for $N = 63$ and $Z = 193$ so that $N + Z = 256 = 2^8$. The plots are only shown for positive values of m since the magnitudes of the far-field beam patterns are symmetric about $m = 0$.

6.5.1 Grating Lobes

Since the far-field beam pattern given by (6.5-1) or, equivalently, (6.5-7) is *periodic* [see (6.5-9)] because the elements are equally spaced, there is a potential problem with *grating lobes*. Grating lobes are *extraneous, unwanted* mainlobes that exist within the visible region. One way to avoid grating lobes is to use unevenly spaced elements. However, since the elements in our linear array are equally spaced, in order to guarantee only one mainlobe within the visible region, steered in the desired direction, the interelement spacing d must be chosen properly.

The criterion that d must satisfy in order to avoid grating lobes can be derived by first substituting (6.5-2) and (6.4-7) into (6.5-1). Doing so yields

$$D(f, f_x) = \mathcal{S}(f) \sum_{n=-N'}^{N'} a_n(f) \exp[j2\pi(f_x - f'_x)nd]. \quad (6.5-20)$$

$$|D_N(f, m)|$$

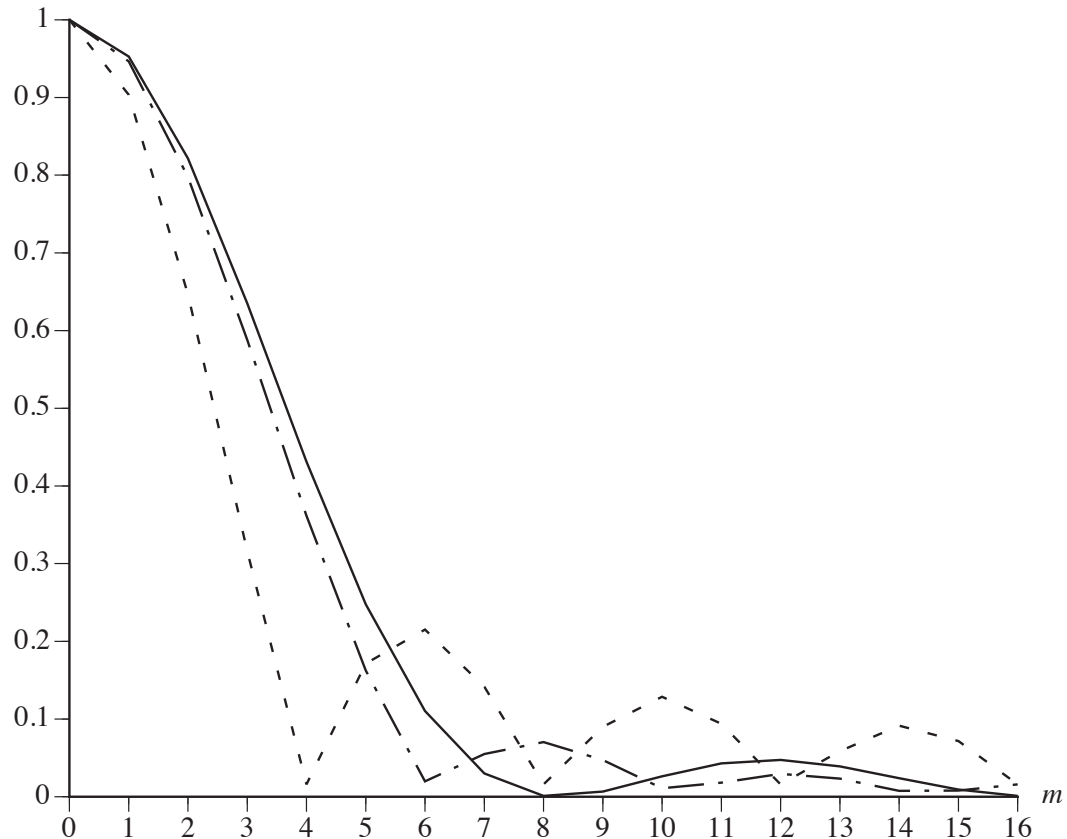


Figure 6.5-1 Magnitudes of the normalized, far-field beam patterns of the rectangular amplitude weights (dashed curve), triangular amplitude weights (solid curve), and cosine amplitude weights (dot-dash curve) plotted as a function of bin number m .

If the amplitude weight $a_n(f) > 0 \quad \forall n$, then the maximum value of the magnitude of (6.5-20) occurs at $f_X = f'_X$ and is given by

$$\begin{aligned}
 D_{\max} &= \max |D(f, f_X)| \\
 &= |D(f, f'_X)| \\
 &= |\mathcal{S}(f)| \sum_{n=-N'}^{N'} a_n(f).
 \end{aligned} \tag{6.5-21}$$

Equation (6.5-21) indicates that the mainlobe of the unnormalized, far-field beam pattern $D(f, f_X)$ has been steered to $f_X = f'_X$. However, the maximum value D_{\max} also occurs at

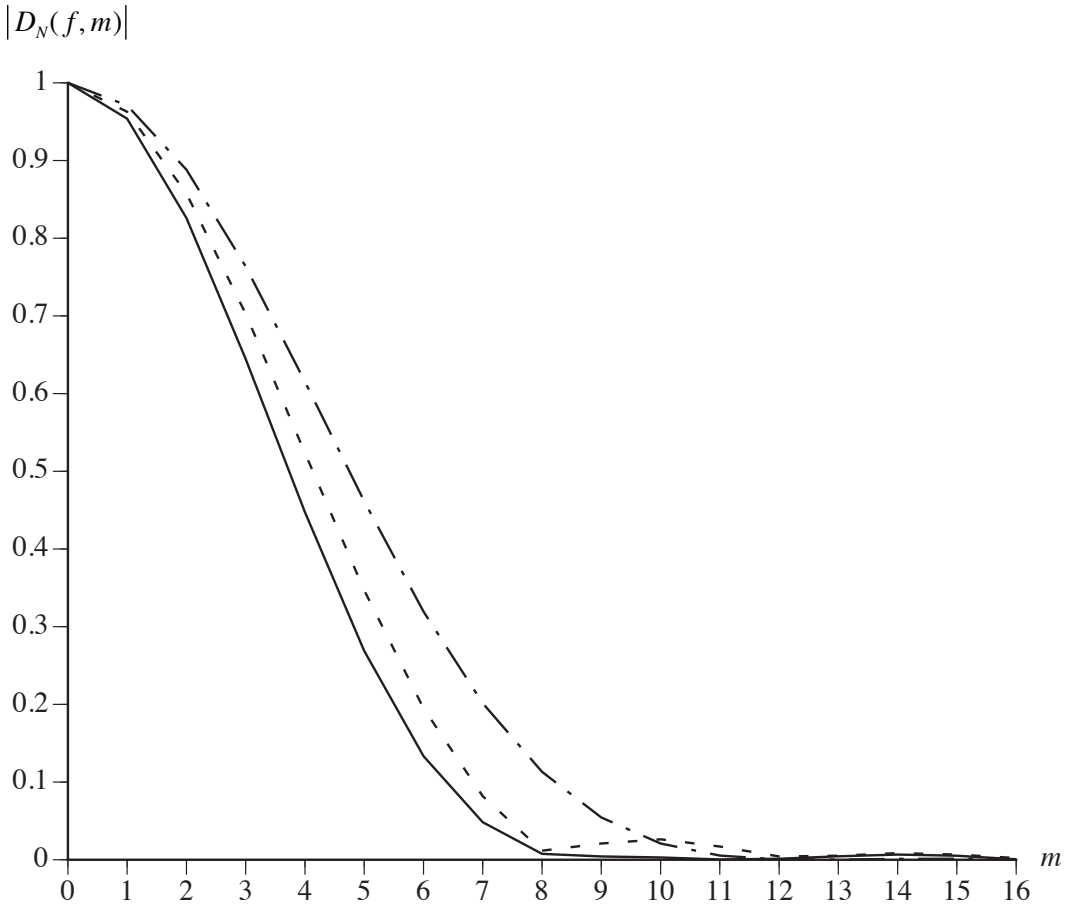


Figure 6.5-2 Magnitudes of the normalized, far-field beam patterns of the Hanning amplitude weights (dashed curve), Hamming amplitude weights (solid curve), and Blackman amplitude weights (dot-dash curve) plotted as a function of bin number m .

$$f_x = f'_x + \frac{i}{d}, \quad i = \pm 1, \pm 2, \pm 3, \dots, \quad (6.5-22)$$

because substituting (6.5-22) into the magnitude of (6.5-20) yields

$$\begin{aligned}
 \left| D\left(f, f'_x + \frac{i}{d}\right) \right| &= |\mathcal{S}(f)| \left| \sum_{n=-N'}^{N'} a_n(f) \exp(+j2\pi in) \right| \\
 &= |\mathcal{S}(f)| \left| \sum_{n=-N'}^{N'} a_n(f) \right| \\
 &= |\mathcal{S}(f)| \sum_{n=-N'}^{N'} a_n(f) \\
 &= D_{\max}, \quad i = \pm 1, \pm 2, \pm 3, \dots
 \end{aligned} \quad (6.5-23)$$

Therefore, if we express (6.5-22) in terms of direction cosines u and u' , then we can state that grating lobes will exist at $u = u_g$, where

$$u_g = u' + i \frac{\lambda}{d}, \quad i = \pm 1, \pm 2, \pm 3, \dots \quad (6.5-24)$$

if $|u_g| \leq 1$, that is, if u_g is in the *visible region*.

If grating lobes can be avoided when a beam pattern is steered to end-fire ($u' = \pm 1$), then grating lobes can be avoided for all possible directions of beam steering. Therefore, if a beam pattern is steered to $u' = 1$, then from (6.5-24), the location of the first possible grating lobe within the visible region occurs when $i = -1$ and is given by

$$u_g = 1 - \frac{\lambda}{d}, \quad i = -1. \quad (6.5-25)$$

If $d < \lambda/2$, then $|u_g| > 1$, which means that *no* grating lobes will exist in the visible region, even if a beam pattern is steered to end-fire. However, since an array must be able to operate over a range of frequencies in general, if

$$d < \lambda_{\min}/2 \quad (6.5-26)$$

where λ_{\min} is the minimum wavelength associated with the maximum frequency $f_{\max} = c/\lambda_{\min}$ in hertz, then *grating lobes will be avoided for all possible directions of beam steering*. If *no* beam steering is done, that is, if $u' = 0$, then grating lobes will be avoided if $d < \lambda_{\min}$.

In order to illustrate grating lobes, consider the magnitude of the normalized, horizontal, far-field beam pattern in the XY plane of a linear array of 7 identical, equally-spaced, rectangular-amplitude-weighted, omnidirectional point-elements lying along the X axis steered to bearing angle ψ' :

$$|D_N(f, 90^\circ, \psi)| = \frac{1}{7} \left| \frac{\sin\left(7\pi \frac{d}{\lambda}(\cos \psi - \cos \psi')\right)}{\sin\left(\pi \frac{d}{\lambda}(\cos \psi - \cos \psi')\right)} \right|, \quad \theta' = 90^\circ. \quad (6.5-27)$$

Figures 6.5-3 and 6.5-4 are polar plots of (6.5-27) for beam-steer angles $\psi' = 45^\circ$ and $\psi' = 0^\circ$ (end-fire), respectively, for $d/\lambda = 1, 0.5$, and 0.45 . **Figure 6.5-3 (b)** shows that for $\psi' = 45^\circ$, $d = \lambda/2$ is sufficient to avoid grating lobes. However,

for $\psi' = 0^\circ$ (end-fire), Fig. 6.5-4 (b) shows that a grating lobe does exist for $d = \lambda/2$, and only when $d < \lambda/2$, does the grating lobe disappear [see Fig. 6.5-4 (c)]. Figures 6.5-3 and 6.5-4 also show that as the ratio d/λ decreases, main-lobe beamwidth increases. Recall from linear aperture theory that main-lobe beamwidth will increase when the frequency (wavelength) is held constant and the length of the aperture is decreased, or when the length of the aperture is held constant and the frequency is decreased (wavelength is increased).

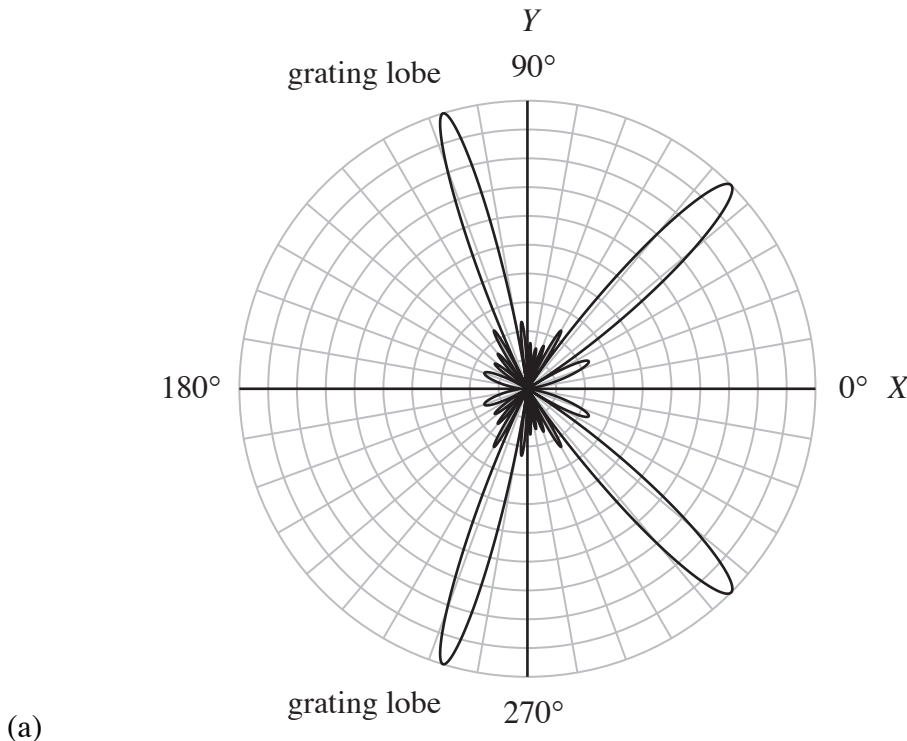
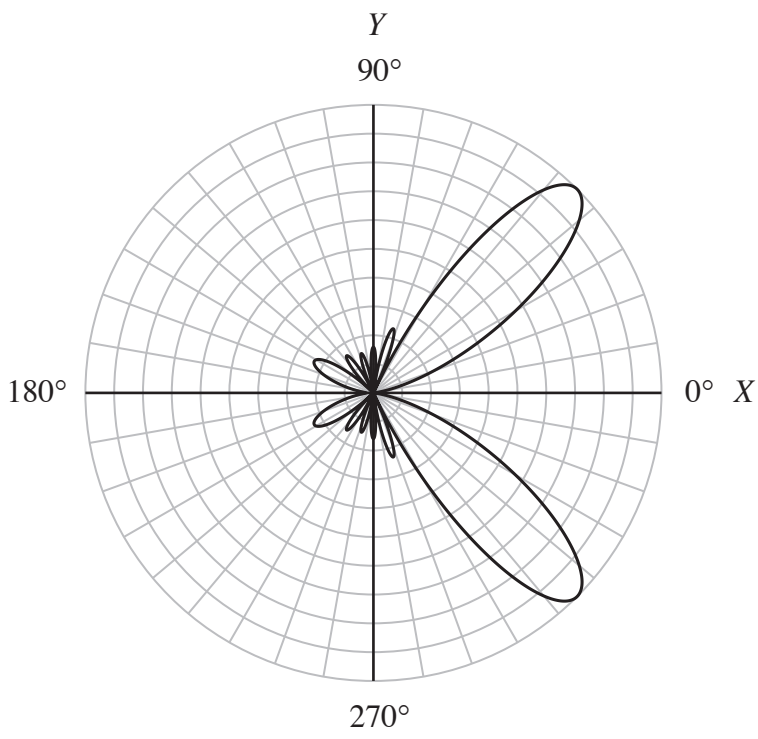


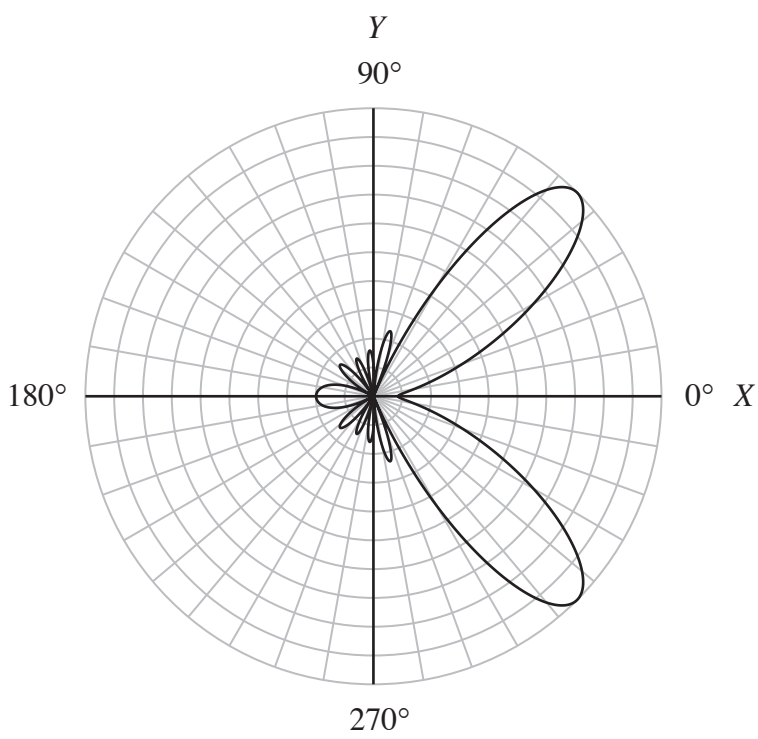
Figure 6.5-3 Polar plots of the magnitudes of the normalized, horizontal, far-field beam patterns of a linear array of $N = 7$ identical, equally-spaced, rectangular-amplitude-weighted, omnidirectional point-elements lying along the X axis for beam-steer angle $\psi' = 45^\circ$ and (a) $d/\lambda = 1$, (b) $d/\lambda = 0.5$, and (c) $d/\lambda = 0.45$.

Example 6.5-1 Spatial-Domain Sampling Theorem

In this example we shall use the *spatial version* of the sampling theorem from time-domain signal processing to derive the criterion that the interelement spacing d must satisfy in order to avoid grating lobes for all possible directions of beam steering. The time-domain sampling theorem states that in order to avoid aliasing, a time-domain signal must be sampled at a rate



(b)



(c)

Figure 6.5-3 *continued.*

$$f_s = \frac{1}{T_s} \geq 2 f_{\max}, \quad (6.5-28)$$

where f_s is the sampling frequency in hertz (or sampling rate in samples per second), T_s is the sampling period in seconds, and f_{\max} is the highest frequency component in hertz contained in the frequency spectrum of the signal. The minimum sampling frequency, $2 f_{\max}$, is known as the Nyquist rate. In practice, it is always recommended to sample at a rate greater than the Nyquist rate.

The *spatial-domain sampling theorem* based on (6.5-28) is given by

$$f_{sx} = \frac{1}{d} \geq 2 \max f_x \quad (6.5-29)$$

where f_{sx} is the spatial sampling frequency in the X direction in cycles per meter

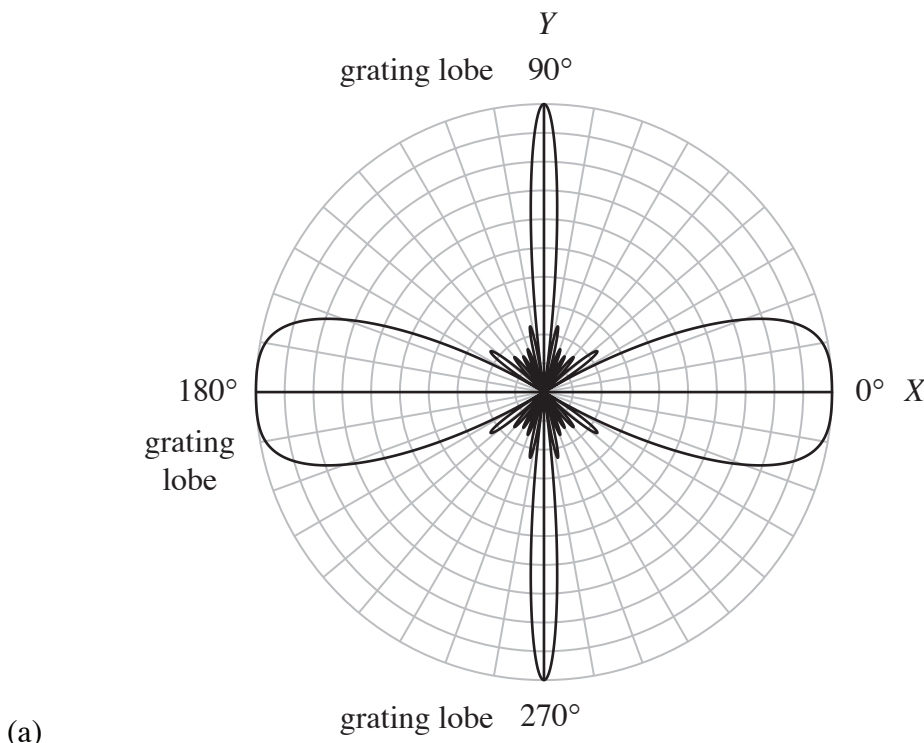


Figure 6.5-4 Polar plots of the magnitudes of the normalized, horizontal, far-field beam patterns of a linear array of $N = 7$ identical, equally-spaced, rectangular-amplitude-weighted, omnidirectional point-elements lying along the X axis for beam-steer angle $\psi' = 0^\circ$ (end-fire) and (a) $d/\lambda = 1$, (b) $d/\lambda = 0.5$, and (c) $d/\lambda = 0.45$.

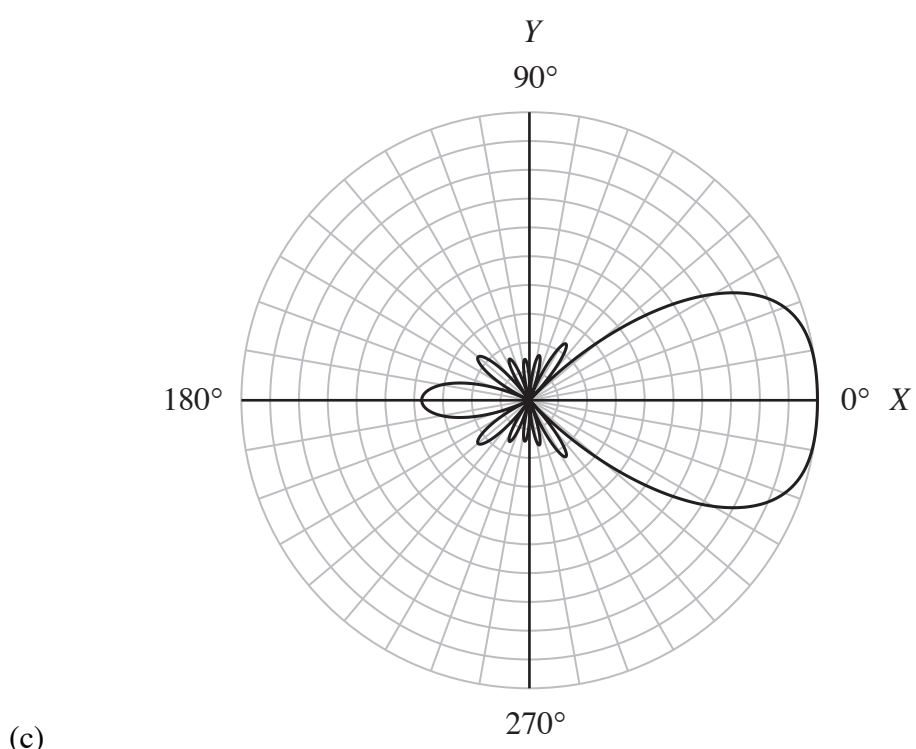
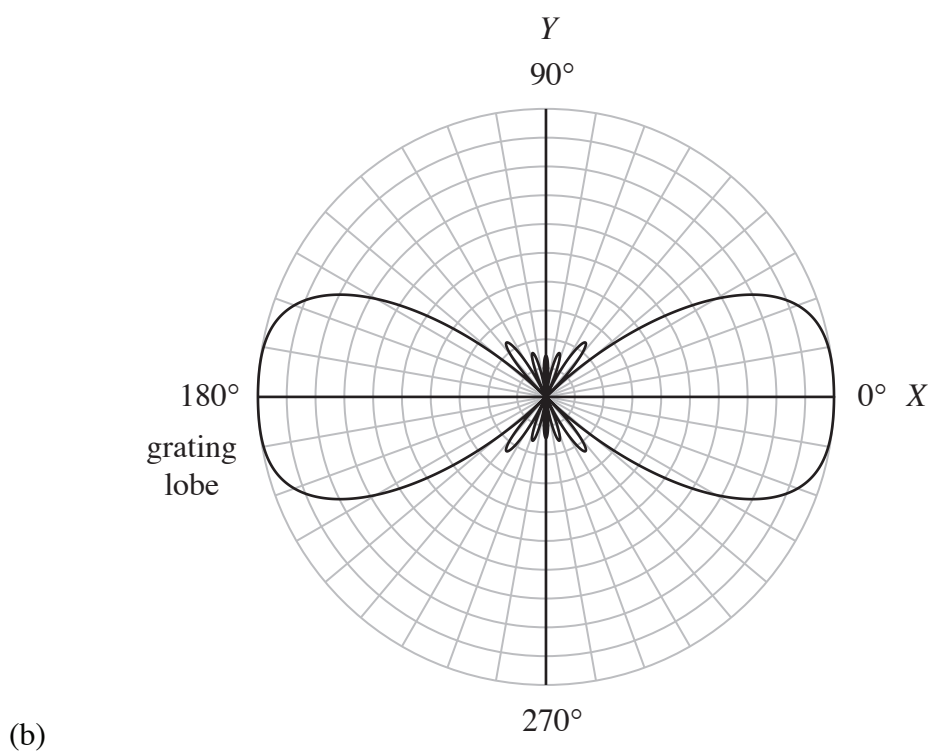


Figure 6.5-4 *continued.*

(a.k.a. the spatial sampling rate in samples per meter), d is the sampling period (interelement spacing) in meters, and $\max f_X$ is the highest spatial-frequency component in the X direction in cycles per meter contained in the spatial Fourier transform (angular spectrum) of a signal that is a function of both time t and spatial coordinate x . For example, a linear array of equally-spaced elements lying along the X axis and being operated in the passive mode samples (measures) acoustic fields incident upon the array every d meters. Therefore, the output electrical signals from the elements are functions of both time and space. Since

$$\max f_X = u_{\max} / \lambda_{\min}, \quad (6.5-30)$$

substituting (6.5-30) into (6.5-29) and setting $u_{\max} = 1$ yields

$$d \leq \lambda_{\min} / 2, \quad (6.5-31)$$

or

$$d < \lambda_{\min} / 2 \quad (6.5-32)$$

where λ_{\min} corresponds to $f_{\max} = c / \lambda_{\min}$, the highest frequency component in hertz contained in the frequency spectrum of the signal. Therefore, if the interelement spacing satisfies (6.5-32) [which is identical to (6.5-26)], then grating lobes will be avoided for all possible directions of beam steering. ■

6.6 The Near-Field Beam Pattern of a Linear Array

As was mentioned at the beginning of [Section 6.1](#), a linear array is an example of a linear aperture. Therefore, the near-field beam pattern (directivity function) of a linear array lying along the X axis is given by the following one-dimensional spatial Fresnel transform (see [Section 2.6](#)):

$$\begin{aligned} \mathcal{D}(f, r, f_X) &= F_{x_A} \left\{ A(f, x_A) \exp \left(-j \frac{k}{2r} x_A^2 \right) \right\} \\ &= \int_{-\infty}^{\infty} A(f, x_A) \exp \left(-j \frac{k}{2r} x_A^2 \right) \exp(+j2\pi f_X x_A) dx_A, \end{aligned} \quad (6.6-1)$$

where $A(f, x_A)$ is the complex frequency response (complex aperture function) of the linear array,

$$k = 2\pi f / c = 2\pi / \lambda \quad (6.6-2)$$

is the wavenumber in radians per meter, and

$$f_x = u/\lambda = \sin\theta \cos\psi/\lambda \quad (6.6-3)$$

is a spatial frequency in the X direction with units of cycles per meter. Since f_x can be expressed in terms of the spherical angles θ and ψ , the near-field beam pattern can ultimately be expressed as a function of frequency f , the range r to a field point, and the spherical angles θ and ψ , that is, $\mathcal{D}(f, r, f_x) \rightarrow \mathcal{D}(f, r, \theta, \psi)$. We shall consider a field point to be in the Fresnel (near-field) region of an array if the Fresnel angle criterion given by either (1.2-35) or (1.2-91) is satisfied, and the range r to the field point – as measured from the center of the array – satisfies the Fresnel range criterion given by

$$1.356R_A < r < \pi R_A^2 / \lambda, \quad (6.6-4)$$

where R_A is the maximum radial extent of the array. If the overall length of the linear array is L_A meters, then $R_A = L_A/2$. Some typical values for the range to the near-field/far-field boundary $r_{\text{NF/FF}} = \pi R_A^2 / \lambda$ for three different frequencies f and two different lengths L_A for a linear towed array are shown in [Table 6.6-1](#), along with values for $r_{\min} = 1.356R_A$.

Table 6.6-1 Values for the Range to the Near-Field/Far-Field Boundary $r_{\text{NF/FF}}$ for a Linear Towed Array

c (m/sec)	f (Hz)	λ (m)	L_A (m)	R_A (m)	r_{\min} (m)	$r_{\text{NF/FF}}$ (km)
1500	60	25.0	100	50	67.8	0.314
1500	100	15.0	100	50	67.8	0.524
1500	1000	1.5	100	50	67.8	5.236
<hr/>						
1500	60	25.0	200	100	135.6	1.257
1500	100	15.0	200	100	135.6	2.094
1500	1000	1.5	200	100	135.6	20.944

If a linear array lies along either the Y or Z axis instead of the X axis, then simply replace x_A and f_x with either y_A and f_y , or z_A and f_z , respectively, in (6.6-1), where spatial frequencies f_y and f_z are given by (1.2-44) and (1.2-45), respectively. As can be seen from (6.6-1), in order to derive the near-field

beam pattern of a linear array, we must first specify a mathematical model for its complex frequency response.

Consider a linear array composed of an odd number N of identical, unevenly-spaced, complex-weighted, omnidirectional point-elements lying along the X axis. The complex frequency response of this array is given by [see (6.1-90)]

$$A(f, x_A) = \mathcal{S}(f) \sum_{n=-N'}^{N'} c_n(f) \delta(x_A - x_n), \quad (6.6-5)$$

where $\mathcal{S}(f)$ is the complex, element sensitivity function (see [Table 6.1-2](#) and [Appendix 6B](#)),

$$c_n(f) = a_n(f) \exp[+j\theta_n(f)], \quad (6.6-6)$$

$$N' = (N-1)/2, \quad (6.6-7)$$

and the impulse function $\delta(x_A - x_n)$ has units of inverse meters. Substituting (6.6-5) into (6.6-1) and making use of the sifting property of impulse functions yields the following expression for the near-field beam pattern:

$$\mathcal{D}(f, r, f_X) = \mathcal{S}(f) \sum_{n=-N'}^{N'} c_n(f) \exp\left(-j \frac{k}{2r} x_n^2\right) \exp(+j2\pi f_X x_n) \quad (6.6-8)$$

If the elements are *equally spaced*, then $x_n = nd$ [see (6.1-91)]. The units of $A(f, x_A)$ and $\mathcal{D}(f, r, f_X)$ are summarized in [Table 6.6-2](#). Equation (6.6-8) is most accurate in the Fresnel region of the linear array where both the Fresnel angle criterion and the Fresnel range criterion are satisfied. It is less accurate in the near-field region outside the Fresnel region where $r < r_{\text{NF/FF}}$, but the Fresnel angle criterion is *not* satisfied. As was discussed in [Subsection 1.2.1](#), the Fresnel region is only a subset of the near-field.

Table 6.6-2 Units of the Complex Frequency Response $A(f, x_A)$ and Corresponding Near-Field Beam Pattern $\mathcal{D}(f, r, f_X)$ for a Linear Array

Linear Array	$A(f, x_A)$	$\mathcal{D}(f, r, f_X)$
active (transmit)	$((m^3/sec)/V)/m$	$(m^3/sec)/V$
passive (receive)	$V/(m^2/sec))/m$	$V/(m^2/sec)$

6.6.1 Beam Steering and Array Focusing

We already know from linear aperture theory that in order to do beam steering and aperture focusing in the Fresnel region of a linear aperture, there must be a linear plus quadratic phase response along the length of the aperture (see [Subsection 2.6.2](#)). A set of phase weights that will produce a linear plus quadratic phase response along the length of the linear array under discussion is given by

$$\theta_n(f) = -2\pi f'_X x_n + \frac{k}{2r'} x_n^2, \quad n = -N', \dots, 0, \dots, N' \quad (6.6-9)$$

where

$$f'_X = u'/\lambda = \sin \theta' \cos \psi' / \lambda \quad (6.6-10)$$

and

$$k = 2\pi f/c = 2\pi/\lambda. \quad (6.6-11)$$

The parameter r' in (6.6-9) is the *focal range*. It is the near-field range from the array where the far-field beam pattern of the array will be in focus. Compare (6.6-9) through (6.6-11) with (2.6-22) through (2.6-26).

If (6.6-6) and (6.6-9) are substituted into (6.6-8), then

$$\mathcal{D}(f, r, f_X) = \mathcal{S}(f) \sum_{n=-N'}^{N'} a_n(f) \exp \left\{ -j \frac{k}{2} \left[\frac{1}{r} - \frac{1}{r'} \right] x_n^2 \right\} \exp [+j 2\pi (f_X - f'_X) x_n], \quad (6.6-12)$$

and if (6.6-12) is evaluated at the near-field range $r = r'$, then it reduces to

$$\mathcal{D}(f, r', f_X) = D(f, f_X - f'_X), \quad (6.6-13)$$

where

$$D(f, f_X) = \mathcal{S}(f) \sum_{n=-N'}^{N'} a_n(f) \exp (+j 2\pi f_X x_n) \quad (6.6-14)$$

is the far-field beam pattern of the array when it is only amplitude weighted. Equation (6.6-13) indicates that the far-field beam pattern $D(f, f_X)$ of the amplitude weights $a_n(f)$ is *in focus* at the near-field range $r = r'$ meters from the array, and has been *steered* in the direction $u = u'$ in direction-cosine space, which is equivalent to steering (tilting) the beam pattern to $\theta = \theta'$ and $\psi = \psi'$

[see (6.6-10)]. However, in the near-field region of the array outside the Fresnel region, a set of quadratic phase weights can only approximately focus the far-field beam pattern. Equal spacing of the elements is *not* required in order to do beam steering and array focusing.

As was discussed in [Section 6.4](#), a phase weight $\theta_n(f)$ in radians is equivalent to a time delay τ'_n in seconds, that is,

$$\theta_n(f) \triangleq -2\pi f \tau'_n, \quad (6.6-15)$$

or

$$\tau'_n = -\theta_n(f)/(2\pi f). \quad (6.6-16)$$

Substituting (6.6-9) through (6.6-11) into (6.6-16) yields

$$\tau'_n = \frac{u'}{c} x_n - \frac{1}{2r'c} x_n^2, \quad n = -N', \dots, 0, \dots, N' \quad (6.6-17)$$

where $c = f\lambda$. The phase weights given by (6.6-9) or, equivalently, the time delays given by (6.6-17) are implemented by using the beamforming procedure shown in [Fig. 6.4-1](#).

Example 6.6-1 Beam Steering and Focusing in the Fresnel (Near-Field) Region

Consider a linear array of 11 identical, equally-spaced, complex-weighted, omnidirectional point-elements lying along the X axis. The array is operated at a frequency of 1 kHz, rectangular amplitude weights are used, the speed of sound $c = 1500$ m/sec, and half-wavelength interelement spacing is used. With the information that is given, we can make the following calculations:

$$N' = \frac{N-1}{2} = \frac{11-1}{2} = 5, \quad (6.6-18)$$

$$\lambda = \frac{c}{f} = \frac{1500 \text{ m/sec}}{1000 \text{ Hz}} = 1.5 \text{ m}, \quad (6.6-19)$$

$$d = \frac{\lambda}{2} = \frac{1.5 \text{ m}}{2} = 0.75 \text{ m}, \quad (6.6-20)$$

the overall length of the array is

$$L_A = (N-1)d = (11-1) \times 0.75 \text{ m} = 7.5 \text{ m} , \quad (6.6-21)$$

and the maximum radial extent of the array is

$$R_A = \frac{L_A}{2} = \frac{7.5 \text{ m}}{2} = 3.75 \text{ m} . \quad (6.6-22)$$

Therefore, the Fresnel region begins at a range of

$$r_{\min} = 1.356 R_A = 1.356 \times 3.75 \text{ m} = 5.085 \text{ m} , \quad (6.6-23)$$

and the range to the near-field/far-field boundary is

$$r_{\text{NF/FF}} = \frac{\pi R_A^2}{\lambda} = \frac{\pi (3.75 \text{ m})^2}{1.5 \text{ m}} = 29.5 \text{ m} . \quad (6.6-24)$$

[Figure 1.2-4](#) illustrates the Fresnel region in the XY plane – in terms of both range and angle – for a linear aperture (linear array) lying along the X axis.

Since

$$f_X = u/\lambda = \sin \theta \cos \psi / \lambda , \quad (6.6-25)$$

$$f'_X = u'/\lambda = \sin \theta' \cos \psi' / \lambda , \quad (6.6-26)$$

and the elements are equally spaced, substituting (6.1-91), (6.6-25), and (6.6-26) into the near-field beam pattern given by (6.6-12) yields

$$\mathcal{D}(f, r, u) = \mathcal{S}(f) \sum_{n=-N'}^{N'} a_n(f) \exp \left\{ -j \frac{k}{2} \left[\frac{1}{r} - \frac{1}{r'} \right] (nd)^2 \right\} \exp \left[+j 2n\pi \frac{d}{\lambda} (u - u') \right] , \quad (6.6-27)$$

or

$$\begin{aligned} \mathcal{D}(f, r, \theta, \psi) = & \mathcal{S}(f) \sum_{n=-N'}^{N'} a_n(f) \exp \left\{ -j \frac{k}{2} \left[\frac{1}{r} - \frac{1}{r'} \right] (nd)^2 \right\} \times \\ & \exp \left[+j 2n\pi \frac{d}{\lambda} (\sin \theta \cos \psi - \sin \theta' \cos \psi') \right] . \end{aligned} \quad (6.6-28)$$

Setting $\theta = 90^\circ$ and $\theta' = 90^\circ$ in (6.6-28) yields

$$\begin{aligned} \mathcal{D}(f, r, 90^\circ, \psi) = & \mathcal{S}(f) \sum_{n=-N'}^{N'} a_n(f) \exp \left\{ -j \frac{k}{2} \left[\frac{1}{r} - \frac{1}{r'} \right] (nd)^2 \right\} \times \\ & \exp \left[+j 2n\pi \frac{d}{\lambda} (\cos \psi - \cos \psi') \right], \quad \theta' = 90^\circ, \end{aligned} \quad (6.6-29)$$

which is the unnormalized, *horizontal*, near-field beam pattern in the *XY* plane of a linear array composed of an odd number N of identical, equally-spaced, complex-weighted, omnidirectional point-elements lying along the *X* axis, with focal range r' and steered to bearing angle ψ' . Equation (6.6-29) is applicable to the array being considered in this example. If quadratic phase weights are *not* used (*no focusing*), then (6.6-29) reduces to

$$\begin{aligned} \mathcal{D}(f, r, 90^\circ, \psi) = & \mathcal{S}(f) \sum_{n=-N'}^{N'} a_n(f) \exp \left[-j \frac{k}{2r} (nd)^2 \right] \times \\ & \exp \left[+j 2n\pi \frac{d}{\lambda} (\cos \psi - \cos \psi') \right], \quad \theta' = 90^\circ. \end{aligned} \quad (6.6-30)$$

Since rectangular amplitude weights are used in this example, $a_n(f) = 1 \quad \forall n$.

Figures 6.6-1 (a), 6.6-2 (a), and 6.6-3 (a) are polar plots of the *normalized* magnitudes of the *unfocused*, horizontal, near-field beam patterns of the array obtained by evaluating (6.6-30) at $r = 8$ m for beam-steer angles $\psi' = 90^\circ$ (broadside), 81° , and 72° (Fresnel angular limit of 18° off broadside), respectively. The magnitude of (6.6-30) was normalized by setting the element sensitivity function $\mathcal{S}(f)$ equal to one and then determining the normalization factor \mathcal{D}_{\max} numerically. Similarly, Figs. 6.6-1 (b), 6.6-2 (b), and 6.6-3 (b) are polar plots of the *normalized* magnitudes of the *focused*, horizontal, near-field beam patterns of the array obtained by evaluating (6.6-29) at $r = 8$ m for $r' = 8$ m and $\psi' = 90^\circ, 81^\circ$, and 72° , respectively. Note that these figures show that the far-field beam pattern of the array has been focused at the near-field range $r = 8$ m and steered. ■

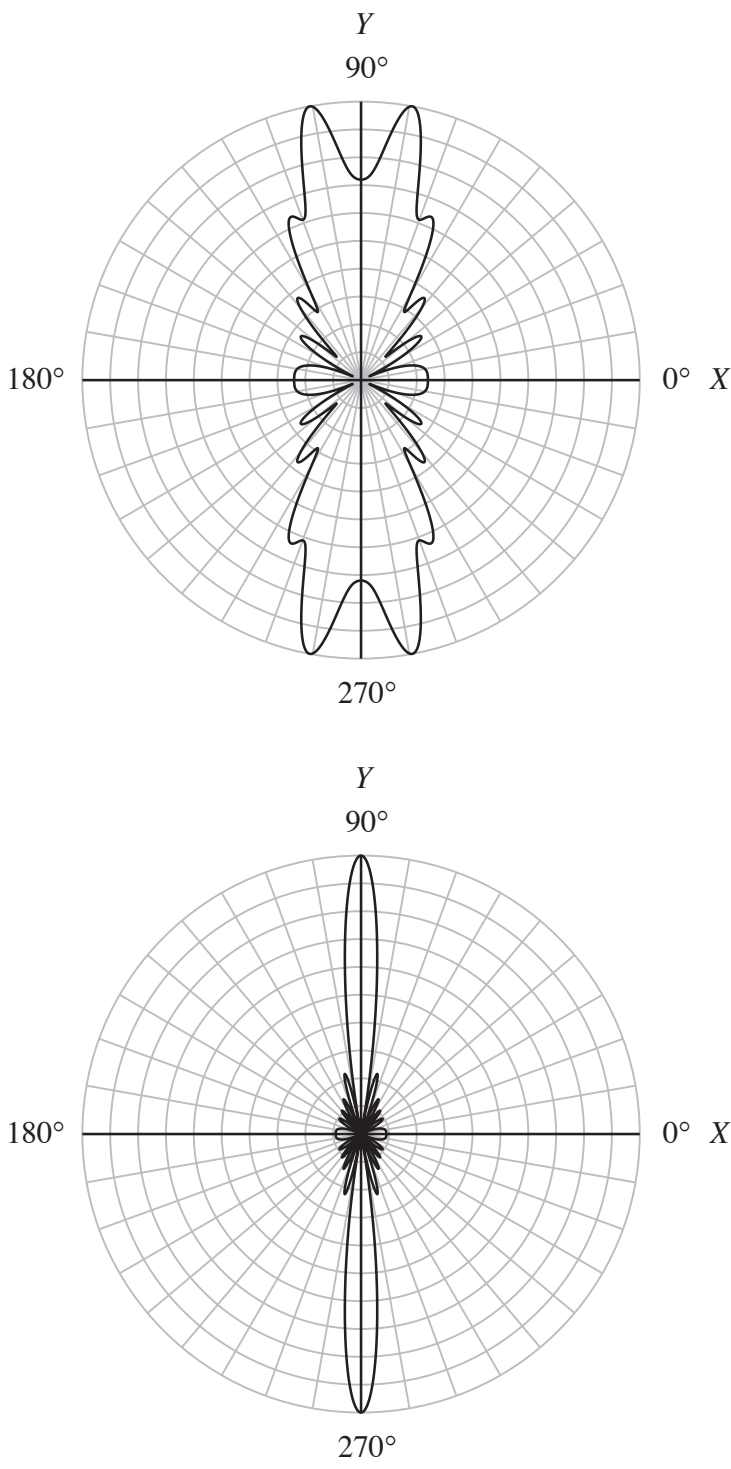


Figure 6.6-1 Polar plots of the normalized magnitudes of the (a) *unfocused* and (b) *focused* horizontal, near-field beam patterns of the array discussed in Example 6.6-1 for beam-steer angle $\psi' = 90^\circ$ (broadside).

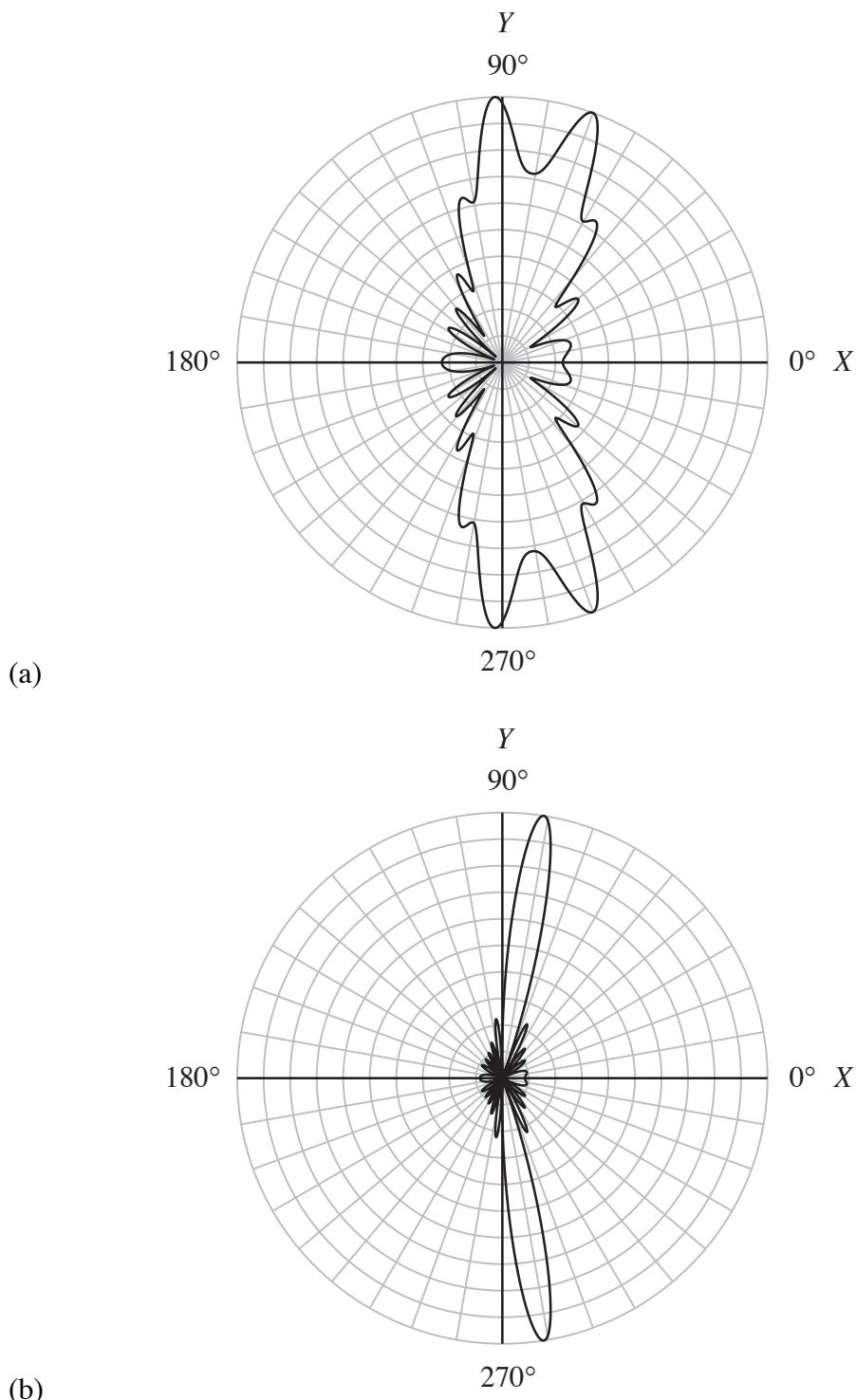


Figure 6.6-2 Polar plots of the normalized magnitudes of the (a) *unfocused* and (b) *focused* horizontal, near-field beam patterns of the array discussed in Example 6.6-1 for beam-steer angle $\psi' = 81^\circ$.

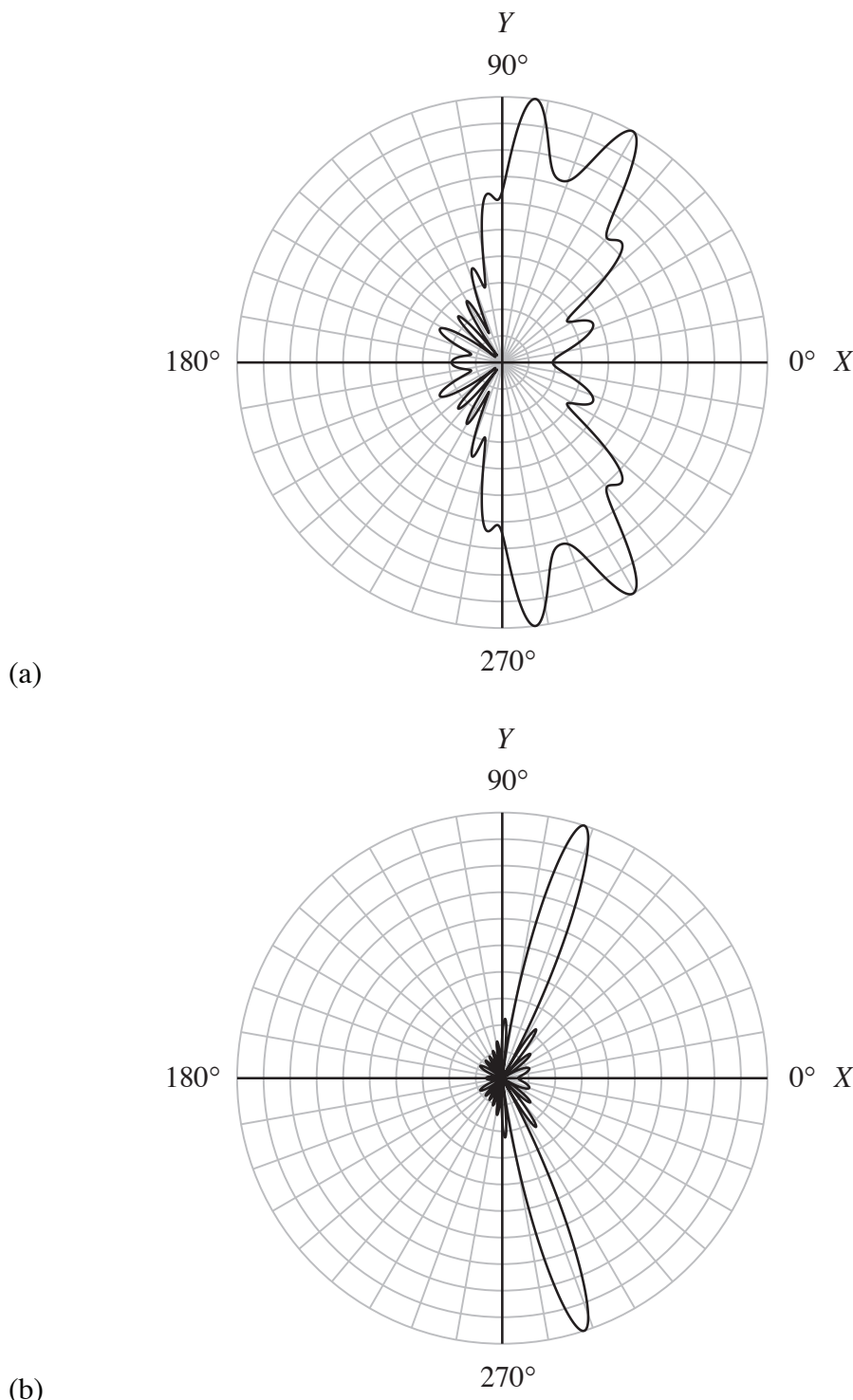


Figure 6.6-3 Polar plots of the normalized magnitudes of the (a) *unfocused* and (b) *focused* horizontal, near-field beam patterns of the array discussed in Example 6.6-1 for beam-steer angle $\psi' = 72^\circ$.

Problems

Section 6.1 Appendix 6B

- 6-1 If the transmitter sensitivity level (transmitting voltage response) of an omnidirectional point-element at 18 kHz is 150 dB re $1 \mu\text{Pa}/\text{V}$ at 1 m , then what is the value of the magnitude of the transmitter sensitivity function in $(\text{m}^3/\text{sec})/\text{V}$? Use $\rho_0 = 1026 \text{ kg/m}^3$ for the ambient density of seawater.
- 6-2 If the receiver sensitivity level (open circuit receiving response) of an omnidirectional point-element at 18 kHz is $-190 \text{ dB re } 1 \text{ V}/\mu\text{Pa}$, then what is the value of the magnitude of the receiver sensitivity function in $\text{V}/(\text{m}^2/\text{sec})$? Use $\rho_0 = 1026 \text{ kg/m}^3$ for the ambient density of seawater.

Section 6.1

- 6-3 Find the unnormalized, far-field beam pattern of a two-element interferometer lying along the (a) Y axis and (b) Z axis as a function of frequency f and spherical angles θ and ψ .
- 6-4 Find the unnormalized, far-field beam pattern of a dipole lying along the (a) Y axis and (b) Z axis as a function of frequency f and spherical angles θ and ψ .
- 6-5 Find the unnormalized, far-field beam pattern of an axial quadrupole lying along the (a) Y axis and (b) Z axis as a function of frequency f and spherical angles θ and ψ .
- 6-6 A linear array composed of an even number N of identical, equally-spaced, complex-weighted, omnidirectional point-elements is lying along the X axis. The complex weights satisfy the conjugate symmetry property given by (6.1-22). The following set of amplitude weights are used: $a_{-n}(f) = a_n(f) = a \quad \forall n$. With the amplitude weights as given, this array can be thought of as a *generalized, two-element interferometer*. Find the unnormalized, far-field beam pattern of this array as a function of frequency f and spatial frequency f_x .
- 6-7 A linear array composed of an even number N of identical, equally-spaced, complex-weighted, omnidirectional point-elements is lying along the X axis. The following set of amplitude and phase weights are used:

$a_n(f) = a$, $a_{-n}(f) = -a_n(f) = -a$, and $\theta_{-n}(f) = -\theta_n(f) \quad \forall n$. Since both the amplitude and phase weights are odd functions of index n , this array can be thought of as a *generalized dipole*. Find the unnormalized, far-field beam pattern of this array as a function of frequency f and spatial frequency f_x .

- 6-8 A linear array composed of an odd number N of identical, equally-spaced, complex-weighted, omnidirectional point-elements is lying along the X axis. The complex weights satisfy the conjugate symmetry property given by (6.1-93). The following set of amplitude weights are used:

$$\begin{aligned} a_{-n}(f) &= a_n(f) = a, & n &= 1, 2, \dots, (N-1)/2 \\ a_0(f) &= -(N-1)a. \end{aligned}$$

With the amplitude weights as given, this array can be thought of as a *generalized axial quadrupole*. Find the unnormalized, far-field beam pattern of this array as a function of frequency f and spatial frequency f_x .

Section 6.2

- 6-9 Show that $S(f, f_x)$ given by (6.2-15) is equal to N at $f_x = 0$ (broadside).

- 6-10 Using the procedure outlined in [Example 2.3-3](#), (a) find the transcendental equation that must be solved in order to compute the dimensionless 3-dB beamwidth Δu in direction-cosine space of the far-field beam pattern given by (6.2-28). (b) If $N = 7$ and $d = \lambda/2$, compute the 3-dB beamwidth $\Delta\psi$ in degrees of the horizontal beam pattern.

Section 6.3

- 6-11 Consider a linear array of 6 identical, equally-spaced elements lying along the X axis, where each element is a single continuous line source or receiver L meters in length. The interelement spacing $d = \lambda/2$ meters.

- (a) Find the set of *normalized* Dolph-Chebyshev amplitude weights so that the magnitude of the level of the mainlobe of the array factor $S(f, f_x)$ is 30 dB above the magnitude of the level of its sidelobes.
- (b) Compute the 3-dB beamwidth $\Delta\psi$ in degrees of the horizontal, angular profile of the array factor $S(f, f_x)$.

- (c) Compute the 3-dB beamwidth $\Delta\theta$ in degrees of the *vertical*, angular profile of the array factor $S(f, f_X)$. Compare $\Delta\theta$ with $\Delta\psi$ from Part (b).

Section 6.4

- 6-12 Consider a linear array composed of an odd number N of identical, equally-spaced, complex-weighted, omnidirectional point-elements. Find the equations for the phase weights and equivalent time delays that will steer the far-field beam pattern of this array to $\theta = 50^\circ$ and $\psi = 112^\circ$ if the array is lying along the
- X axis.
 - Y axis.
- (c) Find the equations for the phase weights and equivalent time delays that will steer the far-field beam pattern of this array to $\theta = 50^\circ$ if the array is lying along the Z axis.
- 6-13 Consider a linear array composed of an *even* number N of identical, *unevenly-spaced*, complex-weighted, omnidirectional point-elements lying along the X axis. Find the equations for the phase weights and equivalent time delays that must be used in order to do beam steering. Also consider the special case of equally-spaced elements.
- 6-14 Find the equations for the phase weights and equivalent time delays that are required in order to steer the mainlobe of the far-field beam pattern of the two-element interferometer discussed in [Example 6.1-1](#).

- 6-15 Find the equations for the phase weights and equivalent time delays that are required in order to steer the far-field beam pattern of the axial quadrupole discussed in [Example 6.1-4](#).

Section 6.5

- 6-16 Verify (6.5-9).
- 6-17 The far-field beam pattern of a linear array of 15 identical, equally-spaced, complex-weighted, omnidirectional point-elements lying along the X axis is computed using a spatial DFT. Half-wavelength interelement spacing is used.
- What is the direction-cosine bin spacing if “padding-with-zeros” is not

done?

- (b) Solve for the number of “zeros” that is required in order to obtain a direction-cosine bin spacing of 0.05 .
- 6-18 Assume that an array must be designed to operate at any one of the following three frequencies: $f = 100, 300$, and 1000 Hz . What criterion must the interelement spacing satisfy in order to avoid grating lobes for all possible directions of beam steering regardless of which frequency is used? Use $c = 1500 \text{ m/sec}$.
- 6-19 Consider a linear array composed of an odd number N of identical, equally-spaced, complex-weighted, omnidirectional point-elements lying along the Z axis. The interelement spacing is d meters (unspecified) and the operating frequency is also unspecified. If you only plan to steer the far-field beam pattern of the array to $\theta' = 45^\circ$ and never to end-fire ($\theta = 0^\circ$ or $\theta = 180^\circ$), then
- (a) what is the location of the *first* possible grating lobe in direction-cosine space?
 - (b) What inequality must d satisfy in order to avoid the first and, thus, all grating lobes?
 - (c) If the operating frequency is 1 kHz and $c = 1500 \text{ m/sec}$, then what inequality must d satisfy?
 - (d) Repeat Parts (a) and (b) for $\theta' = 135^\circ$.

Section 6.6

- 6-20 Consider a linear towed array composed of an odd number N of identical, equally-spaced, complex-weighted, omnidirectional point-elements lying along the X axis. The overall length of the array is 200 m , the operating frequency is 300 Hz , the interelement spacing $d = \lambda/2$ meters, and $c = 1500 \text{ m/sec}$. The spherical coordinates of a sound source (target) as measured from the center of the array are $r_s = 5 \text{ km}$, $\theta_s = 100^\circ$, and $\psi_s = 75^\circ$.
- (a) How many elements are in the array?
 - (b) Is the sound source in the array’s Fresnel region or far-field?
 - (c) What is the equation for the phase weights that must be applied across the array if the array’s far-field beam pattern is to be focused (if

required) and steered to coordinates (r_s, θ_s, ψ_s) ?

(d) What is the equation for the equivalent time delays?

6-21 Consider a linear array composed of an *even* number N of identical, *unevenly-spaced*, complex-weighted, omnidirectional point-elements lying along the X axis.

(a) Find the equation for the near-field beam pattern of this array. Also consider the special case of equally-spaced elements.

(b) What is the equation for the phase weights that must be used in order to do beam steering and array focusing?

(c) What is the equation for the equivalent time delays?

Appendix 6A Normalization Factor for the Array Factor for N Even and Odd

N Even

The general expression for the array factor $S(f, f_X)$ for N even is given by [see (6.1-12)]

$$S(f, f_X) = \sum_{n=1}^{N/2} [c_{-n}(f) \exp(+j2\pi f_X x_{-n}) + c_n(f) \exp(+j2\pi f_X x_n)]. \quad (6A-1)$$

Computing the magnitude of $S(f, f_X)$ yields

$$\begin{aligned} |S(f, f_X)| &= \left| \sum_{n=1}^{N/2} [c_{-n}(f) \exp(+j2\pi f_X x_{-n}) + c_n(f) \exp(+j2\pi f_X x_n)] \right| \\ &\leq \sum_{n=1}^{N/2} |[c_{-n}(f) \exp(+j2\pi f_X x_{-n}) + c_n(f) \exp(+j2\pi f_X x_n)]| \\ &\leq \sum_{n=1}^{N/2} [|c_{-n}(f) \exp(+j2\pi f_X x_{-n})| + |c_n(f) \exp(+j2\pi f_X x_n)|] \\ &\leq \sum_{n=1}^{N/2} [|c_{-n}(f)| |\exp(+j2\pi f_X x_{-n})| + |c_n(f)| |\exp(+j2\pi f_X x_n)|], \end{aligned} \quad (6A-2)$$

which further reduces to

$$|S(f, f_x)| \leq \sum_{n=1}^{N/2} [|a_{-n}(f)| + |a_n(f)|]. \quad (6A-3)$$

Therefore,

$$\max |S(f, f_x)| = \sum_{n=1}^{N/2} [|a_{-n}(f)| + |a_n(f)|]. \quad (6A-4)$$

The absolute value of the real amplitude weights is required because amplitude weights can have both positive and negative values in general.

Equation (6A-4) is the absolute maximum value of $|S(f, f_x)|$. The actual maximum value may be less than (6A-4) as indicated by (6A-3). However, if $a_{-n}(f) > 0$ and $a_n(f) > 0 \forall n$, then the normalization factor S_{\max} for N even is

$$S_{\max} = \max |S(f, f_x)| = \sum_{n=1}^{N/2} [a_{-n}(f) + a_n(f)] \quad (6A-5)$$

Note that if (6A-1) is evaluated at broadside (i.e., at $f_x = 0$) and if no phase weighting is done, then

$$S(f, 0) = \sum_{n=1}^{N/2} [a_{-n}(f) + a_n(f)] \quad (6A-6)$$

and

$$|S(f, 0)| = \left| \sum_{n=1}^{N/2} [a_{-n}(f) + a_n(f)] \right| \leq \sum_{n=1}^{N/2} [|a_{-n}(f)| + |a_n(f)|]. \quad (6A-7)$$

If $a_{-n}(f) > 0$ and $a_n(f) > 0 \forall n$, then

$$|S(f, 0)| = \left| \sum_{n=1}^{N/2} [a_{-n}(f) + a_n(f)] \right| = \sum_{n=1}^{N/2} [a_{-n}(f) + a_n(f)], \quad (6A-8)$$

and by comparing (6A-5) and (6A-8),

$$S_{\max} = \max |S(f, f_x)| = |S(f, 0)| \quad (6A-9)$$

N Odd

The general expression for the array factor $S(f, f_x)$ for N odd is given by [see (6.1-87)]

$$S(f, f_X) = \sum_{n=-N'}^{N'} c_n(f) \exp(+j2\pi f_X x_n). \quad (6A-10)$$

Computing the magnitude of $S(f, f_X)$ yields

$$\begin{aligned} |S(f, f_X)| &= \left| \sum_{n=-N'}^{N'} c_n(f) \exp(+j2\pi f_X x_n) \right| \\ &\leq \sum_{n=-N'}^{N'} |c_n(f) \exp(+j2\pi f_X x_n)| \\ &\leq \sum_{n=-N'}^{N'} |c_n(f)| |\exp(+j2\pi f_X x_n)|, \end{aligned} \quad (6A-11)$$

which further reduces to

$$|S(f, f_X)| \leq \sum_{n=-N'}^{N'} |a_n(f)|. \quad (6A-12)$$

Therefore,

$$\max |S(f, f_X)| = \sum_{n=-N'}^{N'} |a_n(f)|. \quad (6A-13)$$

The absolute value of the real amplitude weights is required because amplitude weights can have both positive and negative values in general.

Equation (6A-13) is the absolute maximum value of $|S(f, f_X)|$. The actual maximum value may be less than (6A-13) as indicated by (6A-12). However, if $a_n(f) > 0 \forall n$, then the normalization factor S_{\max} for N odd is

$$S_{\max} = \max |S(f, f_X)| = \sum_{n=-N'}^{N'} a_n(f) \quad (6A-14)$$

Note that if (6A-10) is evaluated at broadside (i.e., at $f_X = 0$) and if no phase weighting is done, then

$$S(f, 0) = \sum_{n=-N'}^{N'} a_n(f) \quad (6A-15)$$

and

$$|S(f, 0)| = \left| \sum_{n=-N'}^{N'} a_n(f) \right| \leq \sum_{n=-N'}^{N'} |a_n(f)|. \quad (6A-16)$$

If $a_n(f) > 0 \quad \forall n$, then

$$|S(f, 0)| = \left| \sum_{n=-N'}^{N'} a_n(f) \right| = \sum_{n=-N'}^{N'} a_n(f), \quad (6A-17)$$

and by comparing (6A-14) and (6A-17),

$$S_{\max} = \max |S(f, f_x)| = |S(f, 0)| \quad (6A-18)$$

Appendix 6B Transmitter and Receiver Sensitivity Functions of an Omnidirectional Point-Element

Transmitter Sensitivity Function

Manufacturers of electroacoustic transducers usually describe the *transmitting voltage response* of a transducer by plotting the *transmitter sensitivity level* $TSL(f)$ in dB re TS_{ref} at 1 m versus frequency f in hertz. The notation “dB re TS_{ref} ” means decibels relative to a reference transmitter sensitivity. In underwater acoustics, the reference transmitter sensitivity TS_{ref} is usually $1 \mu\text{Pa/V}$. The corresponding *transmitter sensitivity* $TS(f)$ with units of Pa/V is given by

$$TS(f) = TS_{\text{ref}} 10^{[TSL(f)/20]} \quad (6B-1)$$

The transmitter sensitivity $TS(f)$ is a *real, nonnegative* function of frequency.

Values for the magnitude of the transmitter sensitivity function, $|\mathcal{S}_T(f)|$ in $(\text{m}^3/\text{sec})/\text{V}$, for an omnidirectional point-source centered at the origin of a coordinate system, can be obtained from measured values of the transmitter sensitivity, $TS(f)$ in Pa/V , by using the following formula (see [Appendix 6C](#)):

$$|\mathcal{S}_T(f)| = \frac{2r}{f\rho_0} TS(f) \Big|_{r=1 \text{ m}} \quad (6B-2)$$

where

$$r = \sqrt{x^2 + y^2 + z^2} \quad (6B-3)$$

is the distance from the center of the omnidirectional point-source to a field point,

ρ_0 is the constant ambient (equilibrium) density of the fluid medium in kilograms per cubic meter, and $TS(f)$ is given by (6B-1).

Receiver Sensitivity Function

Manufacturers of electroacoustic transducers usually describe the *open circuit receiving response* of a transducer by plotting the *receiver sensitivity level* $RSL(f)$ in dB re RS_{ref} versus frequency f in hertz. The notation “dB re RS_{ref} ” means decibels relative to a reference receiver sensitivity. In underwater acoustics, the reference receiver sensitivity RS_{ref} is usually $1\text{ V}/\mu\text{Pa}$. The corresponding *receiver sensitivity* $RS(f)$ with units of V/Pa is given by

$$RS(f) = RS_{ref} 10^{[RSL(f)/20]} \quad (6B-4)$$

The receiver sensitivity $RS(f)$ is a *real, nonnegative* function of frequency. What we need to do next is to derive the conversion factor that will allow us to convert m^2/sec to Pa for a time-harmonic acoustic field so that values for the magnitude of the receiver sensitivity function, $|\mathcal{S}_R(f)|$ in $\text{V}/(\text{m}^2/\text{sec})$, can be obtained from measured values of the receiver sensitivity $RS(f)$ in V/Pa .

The derivation of the desired conversion factor in this case is simple. By computing the magnitude of (6C-27), we obtain

$$|p_f(\mathbf{r})| = 2\pi f \rho_0 |\varphi_f(\mathbf{r})|, \quad (6B-5)$$

from which we obtain the conversion factor

$$\frac{|p_f(\mathbf{r})|}{|\varphi_f(\mathbf{r})|} = 2\pi f \rho_0 \frac{\text{Pa}}{\text{m}^2/\text{sec}} \quad (6B-6)$$

where $p_f(\mathbf{r}) \equiv p_f(x, y, z)$ and $\varphi_f(\mathbf{r}) \equiv \varphi_f(x, y, z)$. The conversion factor on the right-hand side of (6B-6) is used to convert velocity potential in m^2/sec to acoustic pressure in Pa for a time-harmonic acoustic field. Therefore, values for the magnitude of the receiver sensitivity function, $|\mathcal{S}_R(f)|$ in $\text{V}/(\text{m}^2/\text{sec})$, can be obtained from measured values of the receiver sensitivity, $RS(f)$ in V/Pa , by using the following formula:

$$|\mathcal{S}_R(f)| = 2\pi f \rho_0 RS(f) \quad (6B-7)$$

where ρ_0 is the constant ambient (equilibrium) density of the fluid medium in kilograms per cubic meter and $RS(f)$ is given by (6B-4).

Appendix 6C Radiation from an Omnidirectional Point-Source

An exact solution of the linear wave equation given by (1.2-1) for free-space propagation in an ideal (nonviscous), homogeneous, fluid medium is given by [see (1.2-3)]

$$\varphi(t, \mathbf{r}) = \int_{-\infty}^{\infty} \int_{V_0} X(f, \mathbf{r}_0) A_T(f, \mathbf{r}_0) g_f(\mathbf{r} | \mathbf{r}_0) dV_0 \exp(+j2\pi ft) df, \quad (6C-1)$$

where $\varphi(t, \mathbf{r})$ is the scalar velocity potential in squared meters per second, $X(f, \mathbf{r}_0)$ is the complex frequency spectrum of the input electrical signal at location \mathbf{r}_0 of the transmit aperture with units of volts per hertz, $A_T(f, \mathbf{r}_0)$ is the complex frequency response of the transmit aperture at \mathbf{r}_0 with units of $((m^3/sec)/V)/m^3$,

$$g_f(\mathbf{r} | \mathbf{r}_0) = -\frac{\exp(-jk|\mathbf{r} - \mathbf{r}_0|)}{4\pi|\mathbf{r} - \mathbf{r}_0|} = -\frac{\exp(-jkR)}{4\pi R} \quad (6C-2)$$

is the time-independent, free-space, Green's function of an unbounded, ideal (nonviscous), homogeneous, fluid medium with units of inverse meters,

$$k = 2\pi f/c = 2\pi/\lambda \quad (6C-3)$$

is the wavenumber in radians per meter, $c = f\lambda$ is the constant speed of sound in the fluid medium in meters per second, λ is the wavelength in meters,

$$\mathbf{r} = x\hat{x} + y\hat{y} + z\hat{z} \quad (6C-4)$$

is the position vector to a field point,

$$\mathbf{r}_0 = x_0\hat{x} + y_0\hat{y} + z_0\hat{z} \quad (6C-5)$$

is the position vector to a source point, and

$$R = |\mathbf{r} - \mathbf{r}_0| = \sqrt{(x - x_0)^2 + (y - y_0)^2 + (z - z_0)^2} \quad (6C-6)$$

is the range in meters between a source point and a field point. If an identical

input electrical signal is applied at all locations \mathbf{r}_0 of the transmit aperture, then (see [Example 1.2-1](#))

$$x(t, \mathbf{r}_0) = x(t) \quad (6C-7)$$

and

$$X(f, \mathbf{r}_0) = X(f), \quad (6C-8)$$

where $X(f)$ is the complex frequency spectrum of $x(t)$. Substituting (6C-8) into (6C-1) yields

$$\varphi(t, \mathbf{r}) = \int_{-\infty}^{\infty} X(f) \int_{V_0} A_T(f, \mathbf{r}_0) g_f(\mathbf{r} | \mathbf{r}_0) dV_0 \exp(+j2\pi ft) df. \quad (6C-9)$$

If the transmit aperture is an omnidirectional point-source, then the complex frequency response of the transmit aperture is given by

$$A_T(f, \mathbf{r}_0) = \mathcal{S}_T(f) \delta(\mathbf{r}_0 - \mathbf{r}_s), \quad (6C-10)$$

where $\mathcal{S}_T(f)$ is the complex, *transmitter sensitivity function* of the transducer in $(\text{m}^3/\text{sec})/\text{V}$, and the impulse function $\delta(\mathbf{r}_0 - \mathbf{r}_s)$, with units of inverse cubic meters, represents a unit-amplitude, omnidirectional point-source at $\mathbf{r}_s = (x_s, y_s, z_s)$. Note that $\int_{V_0} A_T(f, \mathbf{r}_0) dV_0 = \mathcal{S}_T(f)$ because $\int_{V_0} \delta(\mathbf{r}_0 - \mathbf{r}_s) dV_0 = 1$.

This result is consistent with the results obtained in [Examples 2B-1](#) and [3B-1](#), that is, integrating the complex frequency response of a transducer over its spatial coordinates yields the complex sensitivity function of the transducer. Substituting (6C-10) into (6C-9) yields

$$\varphi(t, \mathbf{r}) = \int_{-\infty}^{\infty} X(f) \mathcal{S}_T(f) g_f(\mathbf{r} | \mathbf{r}_s) \exp(+j2\pi ft) df \quad (6C-11)$$

where

$$g_f(\mathbf{r} | \mathbf{r}_s) = -\frac{\exp(-jk|\mathbf{r} - \mathbf{r}_s|)}{4\pi|\mathbf{r} - \mathbf{r}_s|} = -\frac{\exp(-jkR)}{4\pi R}, \quad (6C-12)$$

$$\mathbf{r}_s = x_s \hat{x} + y_s \hat{y} + z_s \hat{z} \quad (6C-13)$$

is the position vector to the point-source, and

$$R = |\mathbf{r} - \mathbf{r}_s| = \sqrt{(x - x_s)^2 + (y - y_s)^2 + (z - z_s)^2} \quad (6C-14)$$

is the range in meters between the point-source and a field point. Equation (6C-11) is a general expression for the scalar velocity potential of the acoustic field radiated by an omnidirectional point-source at $\mathbf{r}_s = (x_s, y_s, z_s)$. The corresponding solution for the radiated acoustic pressure $p(t, \mathbf{r})$ in pascals can be obtained by substituting (6C-11) into (1.2-8). Doing so yields

$$p(t, \mathbf{r}) = -j2\pi\rho_0 \int_{-\infty}^{\infty} f X(f) \mathcal{S}_T(f) g_f(\mathbf{r} | \mathbf{r}_s) \exp(+j2\pi ft) df \quad (6C-15)$$

where ρ_0 is the constant ambient (equilibrium) density of the fluid medium in kilograms per cubic meter.

If the input electrical signal is time-harmonic, that is, if (see [Example 1.2-1](#))

$$x(t) = A_x \exp(+j2\pi f_0 t), \quad (6C-16)$$

where A_x is a complex amplitude with units of volts, then

$$X(f) = A_x \delta(f - f_0), \quad (6C-17)$$

where the impulse function $\delta(f - f_0)$ has units of inverse hertz. Substituting (6C-17) into (6C-11) yields

$$\varphi(t, \mathbf{r}) = A_x \mathcal{S}_T(f_0) g_{f_0}(\mathbf{r} | \mathbf{r}_s) \exp(+j2\pi f_0 t), \quad (6C-18)$$

and by replacing f_0 with f ,

$$\varphi(t, \mathbf{r}) = A_x \mathcal{S}_T(f) g_f(\mathbf{r} | \mathbf{r}_s) \exp(+j2\pi ft) \quad (6C-19)$$

or

$$\varphi(t, \mathbf{r}) = \varphi_f(\mathbf{r}) \exp(+j2\pi ft), \quad (6C-20)$$

where

$$\varphi_f(\mathbf{r}) = A_x \mathcal{S}_T(f) g_f(\mathbf{r} | \mathbf{r}_s). \quad (6C-21)$$

Equation (6C-19) is the time-harmonic, scalar velocity potential of the acoustic field radiated by an omnidirectional point-source at $\mathbf{r}_s = (x_s, y_s, z_s)$. The corresponding solution for the time-harmonic, radiated acoustic pressure $p(t, \mathbf{r})$ in pascals is given by

$$p(t, \mathbf{r}) = -j2\pi f \rho_0 A_x \mathcal{S}_T(f) g_f(\mathbf{r} | \mathbf{r}_s) \exp(+j2\pi ft) \quad (6C-22)$$

or

$$p(t, \mathbf{r}) = p_f(\mathbf{r}) \exp(+j2\pi ft), \quad (6C-23)$$

where

$$p_f(\mathbf{r}) = -j2\pi f \rho_0 A_x \mathcal{S}_T(f) g_f(\mathbf{r} | \mathbf{r}_s), \quad (6C-24)$$

or

$$p_f(\mathbf{r}) = -j2\pi f \rho_0 S_0 g_f(\mathbf{r} | \mathbf{r}_s) \quad (6C-25)$$

where

$S_0 = A_x \mathcal{S}_T(f)$

(6C-26)

is the source strength of the omnidirectional point-source in cubic meters per second at frequency f hertz. Note that

$$p_f(\mathbf{r}) = -j2\pi f \rho_0 \varphi_f(\mathbf{r}), \quad (6C-27)$$

where $\varphi_f(\mathbf{r})$ is given by (6C-21).

From (6C-23) it can be seen that

$|p(t, \mathbf{r})| = |p_f(\mathbf{r})|,$

(6C-28)

where from (6C-24)

$|p_f(\mathbf{r})| = \frac{f \rho_0}{2R} |A_x| |\mathcal{S}_T(f)|.$

(6C-29)

Therefore, using (6C-29) to solve for $|\mathcal{S}_T(f)|$ yields

$|\mathcal{S}_T(f)| = \frac{2R}{f \rho_0} \text{TS}(f)$

(6C-30)

where $\mathcal{S}_T(f)$ is the transmitter sensitivity function in $(\text{m}^3/\text{sec})/\text{V}$,

$\text{TS}(f) = |p_f(x, y, z)| / |A_x|$

(6C-31)

is the *transmitter sensitivity* in Pa/V , and the range R is given by (6C-14). If the omnidirectional point-source is placed at the origin of the coordinate system, that

is, if $\mathbf{r}_s = \mathbf{0} = (0, 0, 0)$, then R given by (6C-14) reduces to

$$R = |\mathbf{r}| = r, \quad (6C-32)$$

where

$$r = \sqrt{x^2 + y^2 + z^2}. \quad (6C-33)$$

Evaluating (6C-30) at $R = r = 1$ m yields

$$\boxed{|\mathcal{S}_T(f)| = \frac{2r}{f\rho_0} \text{TS}(f)} \Big|_{r=1\text{ m}} \quad (6C-34)$$

where the range r is given by (6C-33). Note that the range R in (6C-30) and the range r in (6C-34) can be measured in any direction from the center of the omnidirectional point-source.

The magnitude of the source strength can be obtained from (6C-25) as follows:

$$\boxed{|\mathcal{S}_0| = \frac{2R}{f\rho_0} |p_f(x, y, z)|} \quad (6C-35)$$

where the range R is given by (6C-14). If the omnidirectional point-source is placed at the origin of the coordinate system so that $R = r$ [see (6C-32)], then evaluating (6C-35) at $R = r = 1$ m yields

$$\boxed{|\mathcal{S}_0| = \frac{2r}{f\rho_0} |p_f(x, y, z)|} \Big|_{r=1\text{ m}} \quad (6C-36)$$

where the range r is given by (6C-33). Also, from (6C-26),

$$\boxed{|\mathcal{S}_0| = |A_x| |\mathcal{S}_T(f)|} \quad (6C-37)$$

Let us conclude our discussion in this Appendix by deriving the equation for the source distribution $x_M(t, \mathbf{r})$ for a time-harmonic, omnidirectional point-source. The source distribution $x_M(t, \mathbf{r})$, with units of inverse seconds, appears on the right-hand side of the linear wave equation given by (1.2-1). Since the complex frequency spectrum of the source distribution is given by (see Subsection 1.1.1)

$$X_M(f, \mathbf{r}_0) = X(f, \mathbf{r}_0) A_T(f, \mathbf{r}_0), \quad (6C-38)$$

substituting (6C-8), (6C-10), and (6C-17) into (6C-38) yields

$$X_M(f, \mathbf{r}_0) = A_x \mathcal{S}_T(f) \delta(f - f_0) \delta(\mathbf{r}_0 - \mathbf{r}_S). \quad (6C-39)$$

Taking the inverse Fourier transform of (6C-39) yields

$$x_M(t, \mathbf{r}_0) = A_x \mathcal{S}_T(f_0) \delta(\mathbf{r}_0 - \mathbf{r}_S) \exp(+j2\pi f_0 t), \quad (6C-40)$$

and by replacing \mathbf{r}_0 with \mathbf{r} , and f_0 with f , we obtain

$$x_M(t, \mathbf{r}) = A_x \mathcal{S}_T(f) \delta(\mathbf{r} - \mathbf{r}_S) \exp(+j2\pi f t) \quad (6C-41)$$

or

$$x_M(t, \mathbf{r}) = S_0 \delta(\mathbf{r} - \mathbf{r}_S) \exp(+j2\pi f t) \quad (6C-42)$$

where the source strength S_0 is given by (6C-26). Therefore, (6C-19) is an exact solution of the linear wave equation given by (1.2-1) when the source distribution is given by (6C-41), or equivalently, by (6C-42).

Appendix 6D One-Dimensional Spatial FIR Filters

N Even

The Product Theorem for a linear array composed of an even number of identical elements is given by [see (6.1-10)]

$$D(f, f_X) = E(f, f_X) S(f, f_X), \quad (6D-1)$$

where $D(f, f_X)$ is the far-field beam pattern of the array, $E(f, f_X)$ is the far-field beam pattern of *one* of the identical elements in the array, and

$$S(f, f_X) = \sum_{n=1}^{N/2} [c_{-n}(f) \exp(+j2\pi f_X x_{-n}) + c_n(f) \exp(+j2\pi f_X x_n)] \quad (6D-2)$$

is the dimensionless array factor [see (6.1-12)]. Taking the inverse spatial Fourier transform of the Product Theorem given by (6D-1) yields

$$A(f, x_A) = e(f, x_A) * s(f, x_A), \quad (6D-3)$$

where

$$s(f, x_A) = F_{f_X}^{-1}\{S(f, f_X)\} = \sum_{n=1}^{N/2} [c_{-n}(f)\delta(x_A - x_{-n}) + c_n(f)\delta(x_A - x_n)] \quad (6D-4)$$

since

$$F_{f_X}^{-1}\{\exp(+j2\pi f_X x_n)\} = \delta(x_A - x_n). \quad (6D-5)$$

If the elements are omnidirectional point-elements, then the element function $e(f, x_A)$ is given by [see (6.1-14)]

$$e(f, x_A) = \mathcal{S}(f)\delta(x_A), \quad (6D-6)$$

where $\mathcal{S}(f)$ is the element sensitivity function. If we set $\mathcal{S}(f) = 1(m^3/sec)/V$ or $\mathcal{S}(f) = 1V/(m^2/sec)$, then (6D-6) reduces to

$$e(f, x_A) = \delta(x_A). \quad (6D-7)$$

Substituting the “input signal” given by (6D-7) into (6D-3) yields the “output signal”

$$A(f, x_A) = \delta(x_A) * s(f, x_A) = s(f, x_A), \quad (6D-8)$$

where $s(f, x_A)$ given by (6D-4) can be thought of as the spatial impulse response of the array at frequency f hertz. Since (6D-4) is in the form of the impulse response of a finite impulse response (FIR) digital filter, a linear array composed of an even number of identical, complex-weighted elements can be thought of as a one-dimensional, spatial FIR filter.

N Odd

The Product Theorem for a linear array composed of an odd number of identical elements is given by [see (6.1-86)]

$$D(f, f_X) = E(f, f_X)S(f, f_X), \quad (6D-9)$$

where $D(f, f_X)$ is the far-field beam pattern of the array, $E(f, f_X)$ is the far-field beam pattern of *one* of the identical elements in the array, and

$$S(f, f_X) = \sum_{n=-N'}^{N'} c_n(f) \exp(+j2\pi f_X x_n) \quad (6D-10)$$

is the dimensionless array factor [see (6.1-87)]. Taking the inverse spatial Fourier transform of the Product Theorem given by (6D-9) yields

$$A(f, x_A) = e(f, x_A) * s(f, x_A), \quad (6D-11)$$

where, with the use of (6D-5),

$$s(f, x_A) = F_{f_X}^{-1}\{S(f, f_X)\} = \sum_{n=-N'}^{N'} c_n(f) \delta(x_A - x_n). \quad (6D-12)$$

Substituting the “input signal” given by (6D-7) into (6D-11) yields the “output signal”

$$A(f, x_A) = \delta(x_A) * s(f, x_A) = s(f, x_A), \quad (6D-13)$$

where $s(f, x_A)$ given by (6D-12) can be thought of as the spatial impulse response of the array at frequency f hertz. Since (6D-12) is in the form of the impulse response of a finite impulse response (FIR) digital filter, a linear array composed of an odd number of identical, complex-weighted elements can be thought of as a one-dimensional, spatial FIR filter.

Appendix 6E Far-Field Beam Patterns and the Spatial Discrete Fourier Transform for N Even

The far-field beam pattern of a linear array composed of an even number N of identical, equally-spaced, complex-weighted, omnidirectional point-elements lying along the X axis is given by [see (6.1-17)]

$$D(f, f_X) = \mathcal{S}(f) S(f, f_X), \quad (6E-1)$$

where $\mathcal{S}(f)$ is the complex, element sensitivity function, and by substituting (6.1-20) and (6.1-21) into (6.1-12),

$$S(f, f_X) = \sum_{n=1}^{N/2} [c_{-n}(f) \exp[-j2\pi f_X(n-0.5)d] + c_n(f) \exp[j2\pi f_X(n-0.5)d]], \quad (6E-2)$$

or

$$\begin{aligned} S(f, f_X) = & \exp(+j\pi f_X d) \sum_{n=1}^{N/2} c_{-n}(f) \exp(-j2\pi f_X n d) + \\ & \exp(-j\pi f_X d) \sum_{n=1}^{N/2} c_n(f) \exp(+j2\pi f_X n d), \end{aligned} \quad (6E-3)$$

where d is the interelement spacing in meters. Therefore, substituting (6E-3) into (6E-1) yields

$$D(f, f_x) = \mathcal{S}(f) \exp(+j\pi f_x d) \sum_{n=1}^{N/2} c_{-n}(f) \exp(-j2\pi f_x n d) + \\ \mathcal{S}(f) \exp(-j\pi f_x d) \sum_{n=1}^{N/2} c_n(f) \exp(+j2\pi f_x n d). \quad (6E-4)$$

The far-field beam pattern given by (6E-4) can be expressed in terms of two spatial discrete Fourier transforms (DFTs) by appropriately discretizing spatial frequency f_x . Since both summations on the right-hand side of (6E-4) involve only $N/2$ complex weights, f_x is discretized as follows:

$$f_x = m \Delta f_x, \quad m = -N'', \dots, 0, \dots, N'', \quad (6E-5)$$

where

$$\Delta f_x = \frac{1}{(N'+Z)d} \leq \frac{1}{N'd}, \quad (6E-6)$$

$$N' = N/2, \quad (6E-7)$$

and

$$N'' = \begin{cases} (N'+Z)/2, & N'+Z \text{ even}, \\ (N'+Z-1)/2, & N'+Z \text{ odd}. \end{cases} \quad (6E-8)$$

Compare (6E-6) and (6E-8) with (6.5-5) and (6.5-6), respectively, for N odd. Substituting (6E-5) through (6E-7) into (6E-4) yields

$$D(f, m) = \mathcal{S}(f) \left[W_{N'+Z}^{m/2} \sum_{n=1}^{N'} c_{-n}(f) W_{N'+Z}^{-mn} + W_{N'+Z}^{-m/2} \sum_{n=1}^{N'} c_n(f) W_{N'+Z}^{mn} \right], \quad m = -N'', \dots, 0, \dots, N'' \quad (6E-9)$$

where [see (6.5-8)]

$$W_{N'+Z} = \exp\left(+j \frac{2\pi}{N'+Z}\right). \quad (6E-10)$$

The first summation on the right-hand side of (6E-9) is the spatial DFT of the set of $N/2$ complex weights along the negative X axis, whereas the second summation is the spatial DFT of the set of $N/2$ complex weights along the positive X axis. Both spatial DFTs are periodic with period $N'+Z$ because

$$\begin{aligned}
 W_{N'+Z}^{\pm(m+N'+Z)n} &= W_{N'+Z}^{\pm mn} W_{N'+Z}^{\pm(N'+Z)n} \\
 &= W_{N'+Z}^{\pm mn} \exp(\pm j2n\pi) \\
 &= W_{N'+Z}^{\pm mn}.
 \end{aligned} \tag{6E-11}$$

The relationship between bin number m and the corresponding value of direction cosine u_m is given by [see (6.5-13)]

$$u_m = \frac{m}{N'+Z} \frac{\lambda}{d}, \quad m = -N'', \dots, 0, \dots, N'' \tag{6E-12}$$

where N' is given by (6E-7) and N'' is given by (6E-8). If we let δu be the direction-cosine bin spacing, then by using (6E-12)

$$\delta u = u_m - u_{m-1} = \frac{1}{N'+Z} \frac{\lambda}{d}. \tag{6E-13}$$

Solving for Z from (6E-13) yields

$$Z = \frac{1}{\delta u} \frac{\lambda}{d} - N' \tag{6E-14}$$

Equation (6E-14) is used to solve for the number of zeros Z that are required in order to obtain a desired direction-cosine bin spacing δu .

And finally, the normalized, far-field beam pattern $D_N(f, m)$ is given by

$$D_N(f, m) = D(f, m) / D_{\max}, \tag{6E-15}$$

where $D(f, m)$ is the unnormalized, far-field beam pattern given by (6E-9), and if $a_{-n}(f) > 0$ and $a_n(f) > 0 \quad \forall n$, then

$$D_{\max} = \max |D(f, m)| = |\mathcal{S}(f)| \sum_{n=1}^{N/2} [a_{-n}(f) + a_n(f)] \tag{6E-16}$$

is the normalization factor [use the procedure in [Appendix 6A](#) for N even to obtain (6E-16)]. [Figure 6E-1](#) is a plot of the magnitude of (6E-15) using rectangular amplitude weights, $N = 6$, $Z = 125$, and (6E-12) with $d = \lambda/2$. With $N = 6$ and $Z = 125$, $N' = 3$ and $N' + Z = 128 = 2^7$.